Pion-Nucleon Scattering and Pion-Pion Interactions*

J. HAMILTON, P. MENOTTI,† G. C. OADES, AND L. L. J. VICK
Department of Physics, University College, London, England

(Received May 21, 1962)

Low energy s- and p-wave π-N scattering is analyzed by partial wave dispersion relations. From the experimental $\pi-N$ phase shifts we derive the "discrepancies" in the physical energy region and on the crossed cut. We are able to separate the discrepancies into the short-range ($\lesssim 0.2\times10^{-13}$ cm) $\pi-N$ interactions and the $\pi-\pi$ contributions to $\pi-N$ scattering. The $\pi-\pi$ contributions found in this way satisfy several stringent tests which show the validity of our method for deriving and separating the $\pi-\pi$ contributions.

The (+) charge combination of s- and p-wave $\pi-N$ amplitudes yields considerable information about the $T=0$ $\pi-\pi$ interaction at low energies. The $T=0$, $J=0$ $\pi-\pi$ scattering is dominant, and we determine possible sets of the corresponding phase shift $\delta_0{}^0$. Several of our solutions for $\delta_0{}^0$ agree with recent solutions of the Chew-Mandelstam equations for $\pi-\pi$ scattering. Comparison with the latter suggests that the $\pi-\pi$ coupling parameter is $\lambda=-0.18\pm0.05$, and the $\pi-\pi$ scattering length is $a_0=1.3\pm0.4$ (in units where $\hbar=\mu=c=1$). Other information, from the $p+d$ and $\pi+N\to\pi+\pi+N$ experiments and from τ decay, is consistent with our proposed values of $\delta_0{}^0$.

The (−) charge combination of s- and p-wave $\pi-N$ amplitudes gives information about the $T=1$, $J=1$ $\pi-\pi$ interaction which is consistent with the observed ρ resonance. However in the $T=1$, case, complete prediction of our $\pi-N$ results via the helicity amplitudes for $\pi+\pi\to N+\bar{N}$ is not yet satisfactory. Possible reasons for this are given.

The p-wave $\pi-N$ interaction is separated into its constituent parts, and for example, it is seen that any attempt to determine the position of the $(\frac{3}{2},\frac{3}{2})$ resonance must include the $T=0$, $J=0$ $\pi-\pi$ interaction. The extent to which our analysis depends on assuming charge independence is examined. We also discuss how our results can be regarded as a fairly good physical proof of the Mandelstam representation.

1. INTRODUCTION AND SUMMARY

IN earlier papers[1] a method was developed for obtaining information about pion-pion interactions from low-energy pion-nucleon scattering. This was based on the dispersion relations for the partial wave $\pi-N$ amplitudes. In II and III there was a preliminary account of the information about $\pi-\pi$ interactions which was obtained from s-wave $\pi-N$ scattering. In the present paper we give the results of an improved calculation for the s-wave $\pi-N$ case, and in addition give a similar analysis of p-wave $\pi-N$ scattering.

We find that there is a strong low energy attraction between two pions in the $T=0$, $J=0$ state, and that it plays an important part in low-energy s- and p-wave $\pi-N$ scattering. We give values of the $T=0$, $J=0$ $\pi-\pi$ phase shift $\delta_0{}^0$ which reproduce the $\pi-N$ data, and we show how these values compare with values of $\delta_0{}^0$ which have been obtained by several authors from solutions of the Chew-Mandelstam dynamical equations for $\pi-\pi$ scattering. This comparison enables us to give an estimate of the $\pi-\pi$ coupling parameter λ and the $T=0$ s-wave $\pi-\pi$ scattering length a_0. Our results for a_0 and the value of $\delta_0{}^0$ at low energies are compared with other sources of information on $\delta_0{}^0$, such as the $p+d$ experiment, the $\pi+N$ and $\pi+\pi+N$ experiments, and the τ-decay data. It is shown that our results are, by and large, not in disagreement with the theoretical analyses of these experiments. Our analysis gives some evidence for a $T=0$ d-wave $\pi-\pi$ interaction, but it appears to be of no great importance in $\pi-N$ scattering up to 200-MeV lab energy.

The information we obtain about the $T=1$ $\pi-\pi$ interaction is consistent with the effects which would be produced by the ρ resonance (at approximately 760 MeV). There is however some difficulty in calculating the helicity amplitudes for $\pi+\pi\to N+\bar{N}$ in the $T=1$, $J=1$ state. This is probably due to the fact that we have to solve the appropriate Omnès equation for comparatively high energies.

In III we showed how low-energy s-wave $\pi-N$ scattering could be broken down into its constituent contributions from $T=0$ and $T=1$ $\pi-\pi$ interactions, core (short-range) effects, crossed α_{33} resonance effect, and rescattering. Here we do the same for low-energy p-wave $\pi-N$ scattering. In addition to the above effects we have, of course, the long-range Born term in the case of p-wave $\pi-N$ scattering. This breakdown of the p-wave $\pi-N$ scattering gives some interesting results; for example, the $T=0$, $J=0$ $\pi-\pi$ interaction gives an important contribution to the $(\frac{3}{2},\frac{3}{2})$ $\pi-N$ amplitudes, and the position of the $(\frac{3}{2},\frac{3}{2})$ resonance could not be calculated without taking this into account as well as the short-range attraction.

Our analysis of low-energy $\pi-N$ scattering uses the latest values of the phase shifts given by Woolcock.[2] These are partly taken directly from the accurate experimental data, and partly result from an analysis along the lines of Chew, Goldberger, Low, and Nambu[3]. This analysis uses single variable $\pi-N$ dispersion rela-

* This work has been supported in part by the Air Office of Scientific Research, OAR (European Office, Aerospace Research U. S. Air Force).

† On leave of absence from Istituto di Fisica dell'Università, Pisa, Italy.

[1] J. Hamilton and T. D. Spearman, Ann. Phys. (New York) **12**, 172 (1961); J. Hamilton, P. Menotti, T. D. Spearman, and W. S. Woolcock, Nuovo cimento **20**, 519 (1961); J. Hamilton, T. D. Spearman, and W. S. Woolcock, Ann. Phys. (New York) **17**, 1 (1962). These papers will be referred to as I, II, III, respectively.

[2] W. S. Woolcock, *Proceedings of the Aix-en-Provence International Conference on Elementary Particles* (Centre d'Etudes Nucleaires de Saclay, Seine et Oise, 1961), Vol. I, 461.

[3] G. F. Chew, M. L. Goldberger, F. E. Low, and Y. Nambu, Phys. Rev. **106**, 1337 (1957).

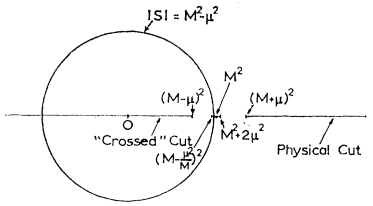

FIG. 1. Location of the pole and cuts of the $\pi-N$ partial wave amplitudes in the complex s plane.

tions for fixed momentum transfer. The $\pi-\pi$ interactions only appear in these relations in the form of subtraction constants, and these subtraction constants are determined by using experimental data. Thus, in no sense are we working in a circle: the $\pi-N$ phase shifts from which we start are directly or effectively experimental values.

The paper is set out as follows. In Sec. 2 the method and evidence for its validity is discussed. In Sec. 3 we derive the $T=0$, $J=0$ phase shifts and in Sec. 4 we discuss the $T=1$ $\pi-\pi$ interaction, and the relation between low energy $\pi-N$ scattering and the nucleon form factors. In Sec. 5 we examine the relation of our results to other information on the $T=0$ and $T=1$ $\pi-\pi$ interactions. There, we also give the breakdown of p-wave $\pi-N$ scattering into its constituent parts, and make some comments on the validity of charge independence and on the validity of the Mandelstam representation.

2. CALCULATION OF THE DISCREPANCIES

(i) The s-Wave π-N Discrepancies

The same notation is used as in III. $s=[(M^2+q^2)^{1/2}+(\mu^2+q^2)^{1/2}]^2$ is the square of the total energy in the c.m. system in the channel $\pi+N\rightarrow\pi+N$. M and μ are the nucleon and pion masses, and q is the momentum in the c.m. system. The s-wave partial $\pi-N$ amplitudes are $f_0^{(T)}(s)$ where $T=\frac{1}{2}, \frac{3}{2}$ is the isotopic spin; these are normalized so that in the elastic region $f_0^{(T)}(s)=e^{i\delta^{(T)}}(\sin\delta^{(T)})/q$, where $\delta^{(T)}$ is the phase shift. We shall use the combinations

$$\begin{aligned} f_0^{(+)}(s)&=\tfrac{1}{2}[f_0^{(\pi-)}(s)+f_0^{(\pi+)}(s)],\\ f_0^{(-)}(s)&=\tfrac{1}{2}[f_0^{(\pi-)}(s)-f_0^{(\pi+)}(s)], \end{aligned} \tag{1}$$

where $f_0^{(\pi-)}(s)$ and $f_0^{(\pi+)}(s)$ are the s-wave scattering amplitudes for $\pi^-+p\rightarrow\pi^-+p$ and $\pi^++p\rightarrow\pi^++p$, respectively.

The Dispersion Relation

The singularities of the partial wave amplitudes as functions of s are shown in Fig. 1. Knowing the position of the singularities we can write down the dispersion relations[4]

$$\begin{aligned} \mathrm{Re}f_0^{(\pm)}(s)=P^{(\pm)}(s)&+\frac{1}{\pi}\int_{(M+\mu)^2}^{\infty}ds'\frac{\mathrm{Im}f_0^{(\pm)}(s')}{s'-s}\\ &+\frac{1}{\pi}\int_0^{(M-\mu)^2}ds'\frac{\mathrm{Im}f_0^{(\pm)}(s')}{s'-s}+\Delta_0^{(\pm)}(s), \end{aligned} \tag{2}$$

where s lies either on the physical cut $(M+\mu)^2\leqslant s\leqslant\infty$ or on the "crossed cut" $0\leqslant s\leqslant(M-\mu)^2$. One of the integrals on the right will be singular and it has to be evaluated as a principal value integral. $P^{(\pm)}(s)$ denotes the sum of those Born terms which arise from the pole $s'=M^2$ and the short cut $(M-\mu^2/M)^2\leqslant s'\leqslant M^2+2\mu^2$. We call the first integral on the right of (2) the physical integral and the second integral will be called the crossed integral. The physical integral gives the contribution to $\mathrm{Re}f_0(s)$ due to rescattering, and the crossed integral gives the effect of the crossed graphs. The $(\frac{3}{2},\frac{3}{2})$ and the higher $\pi-N$ resonances contribute to the s-wave $\pi-N$ amplitude through the crossed integral.

We call $\Delta_0^{(\pm)}(s)$ the s-wave discrepancies. These are made up of the contributions to (2) arising from the far unphysical cut $-\infty\leqslant s'\leqslant 0$ and the circle $|s'|=M^2-\mu^2$. The former is equivalent to $\pi-N$ interactions of range[5] $\lesssim\hbar/Mc$, while the circle arises solely from the channel $\pi+\pi\rightarrow N+\bar{N}$. The left half of the circle also is equivalent to short-range interactions (range $\leqslant\hbar/Mc$). The right half of the circle, and in particular the part near $s'=M^2-\mu^2$, gives a comparatively long-range interaction between the pion and the nucleon which is due to low-energy $\pi-\pi$ scattering.

We evaluate $\Delta_0^{(\pm)}(s)$ in the physical region $s\geqslant(M+\mu)^2$ by substituting the known s-wave $\pi-N$ phase shifts on the left of (2) and in the physical integral on the right. The Born terms $P^{(\pm)}(s)$ are calculated using the coupling constant $f^2=0.081$ (these Born terms are very small in the s-wave case, as was shown in I). The crossed integral is evaluated by means of the crossing theorem using known s-wave, p-wave, $\cdots$ $\pi-N$ phase shifts and using certain information about high-energy $\pi-N$ scattering.[6] Equation (2) then yields $\Delta_0^{(\pm)}(s)$.

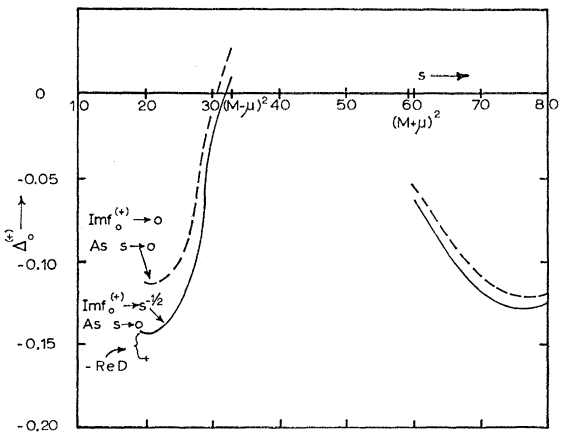

FIG. 2. The discrepancy $\Delta_0^{(+)}(s)$ for s-wave $\pi-N$ scattering. The solid curve is obtained by assuming $\mathrm{Im}f_0^{(+)}(s)$ behaves like $s^{-1/2}$ as $s\rightarrow 0$, and the broken curve is obtained by assuming $\mathrm{Im}f_0^{(+)}(s)\rightarrow 0$ as $s\rightarrow 0$. The cross at $s=20$ indicates where the solid curve would end if we neglected d waves.

[4] For a discussion of convergence and possible subtractions see III, Sec. V (ii).

[5] For a definition of the range of the equivalent interaction, see III, Sec. I (ii).

[6] For details see III.

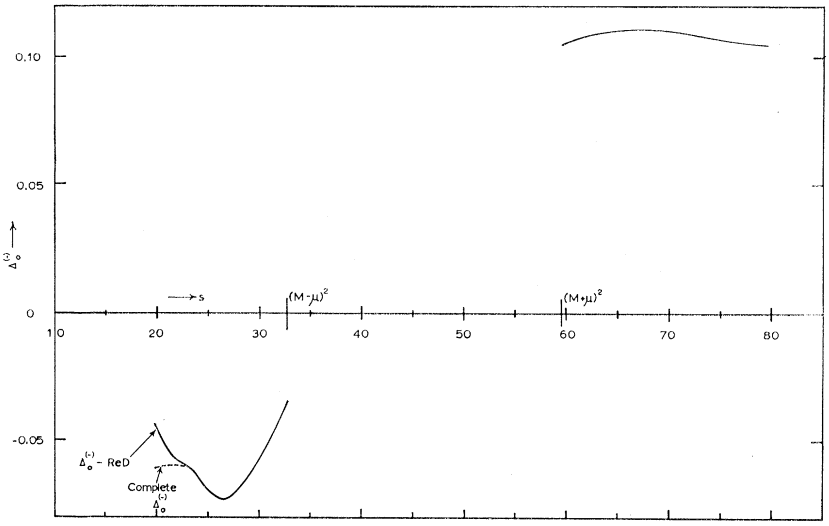

FIG. 3. The discrepancy $\Delta_0^{(-)}(s)$ for s-wave $\pi-N$ scattering. The broken line for $s<23$ shows the effect of the d waves.

Applying the crossing theorem to $\mathrm{Re}f_0^{(\pm)}(s)$, we can also evaluate $\Delta_0^{(\pm)}(s)$ on the right-hand part of the "crossed cut" $0\leqslant s\leqslant(M-\mu)^2$. In practice the accuracy of this calculation is limited by our knowledge of the $\pi-N$ scattering phase shifts at moderate and high energies. We have carried out the calculation for $20\mu^2\leqslant s\leqslant(M-\mu)^2=32.7\mu^2$, and our results are quite reliable for $25\mu^2\leqslant s\leqslant 32.7\mu^2$.

Separation of the Low-Energy $\pi-\pi$ Effects

We have seen that the effect of low-energy $\pi-\pi$ interactions on $\pi-N$ scattering comes from the front of the circle $|s'|=M^2-\mu^2$ (i.e., the part nearest $s'=M^2-\mu^2$). This will result in a fairly rapid variation of $\Delta_0^{(\pm)}(s)$ with s over the range of values of s where we have calculated it. The remainder of $\Delta_0^{(\pm)}(s)$ comes from the more distant parts of the cuts and is expected to be a slowly varying function of s over the range of our calculation. In fact this remaining part of $\Delta_0^{(\pm)}(s)$ should be well approximated by a constant[7] plus a single pole somewhere on the cut $-\infty\leqslant s'\leqslant 0$. This part of $\Delta_0^{(\pm)}(s)$ is due to the short-range part of the $\pi-N$ interaction, and we shall call it the core interaction (the corresponding range of interaction is $\lesssim\hbar/Mc$).

This interpretation of $\Delta_0^{(\pm)}(s)$ is supported by certain symmetry properties which were derived in II. In particular the low-energy $\pi-\pi$ part of $\Delta_0^{(+)}(s)$ is expected to be approximately of the form

$$\frac{(\text{const})}{(s-\mathrm{Re}s_1)^2+(\mathrm{Im}s_1)^2}, \tag{3}$$

where[8] $s_1\simeq(M^2-\mu^2)e^{i\phi_1}$ and ϕ_1 is some angle less than about 35°. Figure 2 shows the calculated values of $\Delta_0^{(+)}(s)$. Clearly it is well represented by the form (3) plus a term which varies slowly with s. The low-energy $\pi-\pi$ part of $\Delta_0^{(-)}(s)$ is similarly expected to be approximately of the form

$$\frac{(\text{const})(s-\mathrm{Re}s_1')}{(s-\mathrm{Re}s_1')^2+(\mathrm{Im}s_1')^2}, \tag{4}$$

where s_1' is defined in the same way as s_1 above. Figure 3 shows the calculated values of $\Delta_0^{(-)}(s)$. Expansion (4) plus a constant gives a rough approximation to the form of $\Delta_0^{(-)}(s)$. In particular, it explains the noticeable difference between the values of $\Delta_0^{(-)}(s)$ for $s\leqslant(M-\mu)^2$ and its values for $s\geqslant(M+\mu)^2$. It is also shown in II that if the $\pi-\pi$ interaction in the isotopic spin state $T=1$ is only appreciable for moderate, but not low, $\pi-\pi$ energies, say for $t\gtrsim 20\mu^2$ where t is the square of the energy of the $\pi-\pi$ state in its c.m. system, then (4) is only a rough approximation to the $\pi-\pi$ part of $\Delta_0^{(-)}(s)$. Comparison of (4) with Fig. 3 suggests that this is, indeed, the case.

In the present paper we improve considerably on the information which can be obtained using (3) and (4). Various forms of the s-wave $\pi-\pi$ phase shift $\delta_0^0(t)$ are used to calculate the low-energy $\pi-\pi$ part of $\Delta_0^{(+)}(s)$. Adding a slowly varying function of s and comparing the result with Fig. 2, we can determine the s-wave $\pi-\pi$ scattering length, etc. As a check on our results we can require the same s-wave $\pi-\pi$ phase shifts to give agreement between the theoretical and the calculated values of the discrepancies $\Delta_{1/2}^{(+)}(s)$ and $\Delta_{3/2}^{(+)}(s)$ in the dispersion relation for p-wave $\pi-N$ scattering (cf. Sec. 3). We similarly fit the $\Delta_0^{(-)}(s)$ curve in Fig. 3 by assuming various resonances in the $T=1$, $J=1$ $\pi-\pi$ system, and again a check on our results is given by the requirement of also fitting the p-wave $\pi-N$ discrepancies $\Delta_{1/2}^{(-)}(s)$ and $\Delta_{3/2}^{(-)}(s)$.

$\pi-N$ Phase Shift Data Used

The new values of $\Delta_0^{(+)}(s)$ and $\Delta_0^{(-)}(s)$ shown in Figs. 2 and 3 are in several ways superior to the values

[7] The constant arises from the far unphysical region, where s' is large and negative.

[8] Note that $M^2\cong 45\mu^2$.

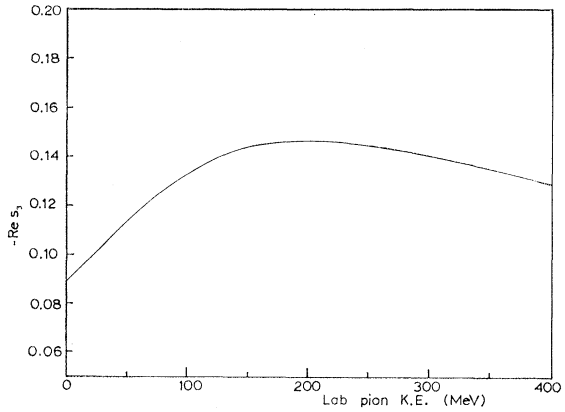

FIG. 4. Values of the $\pi-N$ s-wave amplitude $\mathrm{Re}s_3=(\sin 2\alpha_3)/2q$ where q is the momentum in the c.m. system.

given in II and III. The range of s in the physical region has been extended to $59.6=(M+\mu)^2\leqslant s\leqslant 80$ (we use units $\hbar=\mu=c=1$ throughout), i.e., from threshold to pion (lab) energy 215 MeV. In the crossed region the range is $20\leqslant s\leqslant 32.7=(M-\mu)^2$.

s-wave $\pi-N$ shifts. In the original calculation two sets of discrepancies were given because of ambiguities in the high-energy values of the s-wave $\pi-N$ phase shifts α_1 and α_3. In the present calculation Woolcock's[9] values for these phase shifts up to 400 MeV are used. These values are given in Figs. 4 and 5. Woolcock's values of α_1 and α_3 (and of the small p-wave phase shifts discussed below) are derived partly from an improved form of the dispersion relation method of Chew *et al.*,[10] and partly from certain particularly accurate experimental phase shift determinations. The α_3 plot shown in Fig. 4 passes through, or close to the accurate experimental values at 31, 98, 120, 224, and 310 MeV. The α_1 plot in Fig. 5 passes through or close to the accurate experimental values at 31, 98, 120, and 224 MeV. Above 250 MeV Woolcock's values of α_1 lie about half way between the two sets of values of α_1 used in II and III.

Woolcock's values give us $\mathrm{Re}f_0^{(\pm)}(s)$ with considerable accuracy in $59.6\leqslant s\leqslant 80$ (i.e., for lab energies up to 215 MeV). For the physical integral and the crossed integral we require $\mathrm{Im}f_0^{(\pm)}(s)$ at higher energies. Above 2 BeV we use the value $\mathrm{Im}f_0^{(T)}=0.22/q$ as suggested by the partially opaque optical disk [cf. Eq. (9) of III]; here $T=\frac{1}{2}$, $\frac{3}{2}$ is the isotopic spin. Between 400 MeV and 2 BeV we join up $\mathrm{Im}f_0^{(\pm)}(s)$ with smooth curves. As was pointed out in III, the errors arising from our rough approximations above 400 MeV are likely to raise or lower the $\Delta_0^{(\pm)}(s)$ curves bodily, but should not tilt or deform them appreciably.

In calculating $\mathrm{Re}f_0^{(\pm)}(s)$ and $\mathrm{Im}f_0^{(\pm)}(s)$ in the crossed region $s\leqslant 32.7$ we require the p-wave and possibly some d-wave $\pi-N$ phase shifts as well as the s-wave phase shifts. From Table IV of III it is seen that to find $f_0^{(\pm)}(s)$ in $25\leqslant s\leqslant 32.7$ we require these phase shifts up to 200 MeV, and for $20\leqslant s\leqslant 32.7$ we require them up to 400 MeV. We shall not place much reliance on $\Delta_0^{(\pm)}(s)$ in $20\leqslant s\leqslant 25$.

p-wave $\pi-N$ phase shifts. The main contributions to $\Delta_0^{(\pm)}(s)$ from α_{33} come from the region of the $(\frac{3}{2},\frac{3}{2})$ resonance, and small errors in α_{33} away from the resonance are relatively unimportant. For convenience of calculation simple parametric fits were used for α_{33}. Below the $(\frac{3}{2},\frac{3}{2})$ resonance α_{33} was expressed in a simple power series in q, so as to give agreement with Woolcock's value of the scattering length α_{33} [see Eq. (16) below] and the accurate experimental data. Above the resonance another simple parametric form was used. This gave good agreement with the accurate experimental values such as that at 310 MeV.[11] The values of α_{33} used in calculating $\Delta_0^{(\pm)}(s)$ are shown in Fig. 6. It should be noted that any inaccuracies in $\Delta_0^{(\pm)}(s)$ due to the kink in α_{33} just above the resonance will only be noticeable for $20\leqslant s\leqslant 23$, i.e., at the very lower end of our range. It should also be noted that in calculating the p-wave $\pi-N$ discrepancies it was necessary to use a more accurate set of values for α_{33}. These are described in Sec. 2(ii) below.

The α_{33} phase shift is the predominant p-wave effect in $\Delta_0^{(\pm)}(s)$ for $s\leqslant 32.7$. However we also included the small p-wave phase shifts α_{11}, α_{13}, α_{31}. For these we used the values calculated with great care by Woolcock up to 400 MeV.[9] Figure 7 shows the values up to 100 MeV. They are in fairly good agreement with accurate experimental values at 31, 98, and 120 MeV(α_{31}),[12–14]

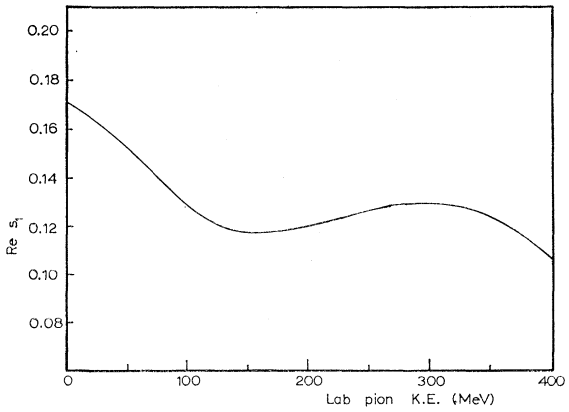

FIG. 5.

FIG. 5. Values of the $\pi-N$ s-wave amplitude $\mathrm{Re}s_1=(\sin 2\alpha_1)/2q$ where q is the momentum in the c.m. system.

[9] W. S. Woolcock, Ph.D. thesis, Cambridge University, 1961 (unpublished); and *Proceedings of the Aix-en-Provence Conference on High-Energy Physics* (Centre d'Etudes Nucleaires de Saclay, Seine et Oise, 1961). See also J. Hamilton and W. S. Woolcock (to be published). We are indebted to Dr. Woolcock for permission to quote his results and reproduce Figs. 4, 5, and 7.

[10] G. F. Chew, M. L. Goldberger, F. E. Low, and Y. Nambu, Phys. Rev. **106**, 1337 (1957).

[11] J. H. Foote, O. Chamberlain, E. H. Rogers, and H. M. Steiner, Phys. Rev. **122**, 959 (1961).

[12] Rochester University result (Set I). We are indebted to Dr.

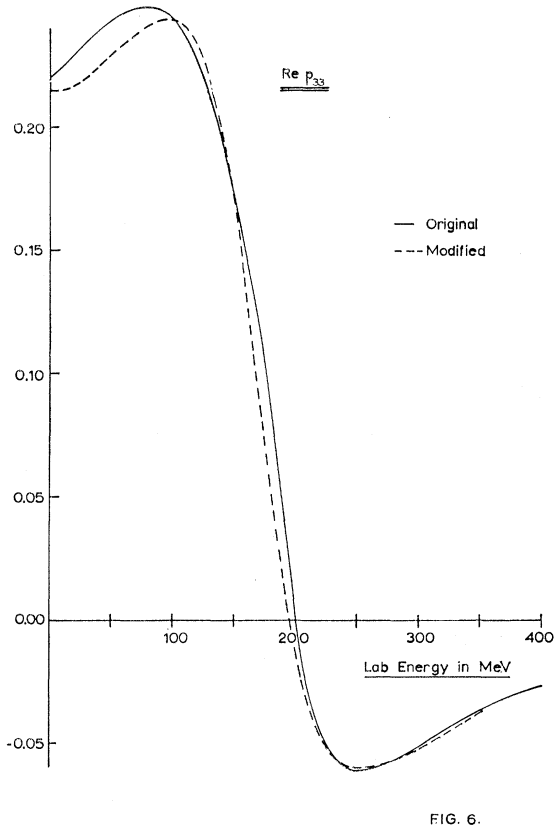

FIG. 6.

FIG. 6. Values of $\mathrm{Re}p_{33}=(\sin 2\alpha_{33})/2q^3$, where q is the momentum in the c.m. system. The broken line shows the values used in Sec. 2 (ii).

and are consistent with measurements at 224 MeV.[15] The curves in Fig. 7 are also in agreement with Woolcock's[9] values for the p-wave scattering lengths [Eq. (16) below] which are a best fit obtained from a variety of distinct methods. So far as $\Delta_0^{(\pm)}(s)$ are concerned we can safely ignore any errors in these small p-wave $\pi-N$ phase shifts. For higher energies (above 400 MeV) the absorptive part of the p-wave amplitudes is joined smoothly on to the form $0.22/q$ which is used above 2 BeV. Errors here will not affect our analysis of $\Delta_0^{(\pm)}(s)$.

d-wave $\pi-N$ phase shifts. We can neglect these except for δ_{13} which contributes to $\mathrm{Im}f_0^{(\pm)}(s)$ for the small values of s. We assumed that the 600-MeV $\pi-N$ resonance is an almost elastic[16] $T=\frac{1}{2}$, $D_{3/2}$ state, and the resonant part of the total cross section $\sigma_{\pi-p}$ was estimated. The values of δ_{13} below the resonance were estimated partly from the width of the resonance and partly from Woolcock's[9] low-energy values of δ_{13}. Figures 2 and 3 show that the δ_{13} contribution to $\Delta_0^{(\pm)}(s)$ is only appreciable for $s<23$.

In evaluating the crossed integral for $\Delta_0^{(+)}(s)$ the unknown behavior of $\mathrm{Im}f_0^{(+)}(s')$ as $s'\to 0$ might appear to give rise to difficulty. As was pointed out in III, this behavior is related to backward $\pi-N$ scattering at very high energy, and it is tied up with the question whether the neutron behaves like a Regge pole in these circumstances. The discrepancy $\Delta_0^{(+)}(s)$ was calculated for the two assumptions $\mathrm{Im}f_0^{(+)}(s')\to 0$ as $s'\to 0$ and $\mathrm{Im}f_0^{(+)}(s')\sim(s')^{-1/2}$ as $s'\to 0$. The resulting values of $\Delta_0^{(+)}(s)$ are shown in Fig. 2; the difference between them is unimportant.

The errors in the calculation of the s-wave discrepancies $\Delta_0^{(\pm)}(s)$ have been discussed in detail in III; the errors in the new values of $\Delta_0^{(\pm)}(s)$ are certainly no greater than those given in III.

(ii) The p-Wave Discrepancies $\Delta_{1/2}{}^{(\pm)}(s)$ and $\Delta_{3/2}{}^{(\pm)}(s)$

Let $f_{1-}{}^{(T)}(s)$ and $f_{1+}{}^{(T)}(s)$ be the p-wave $\pi-N$ partial amplitudes for the states with angular momentum $J=\frac{1}{2}$ and $J=\frac{3}{2}$, respectively ($T=\frac{1}{2}$, $\frac{3}{2}$ is the isotopic spin). We use the amplitudes $p_{2T,1}\equiv f_{1-}{}^{(T)}(s)/q^2$ and $p_{2T,3}\equiv f_{1+}{}^{(T)}(s)/q^2$. These amplitudes $p_{2T,2J}$ obey dispersion relations of the same form as (2). They are

$$\mathrm{Re}p_{2T,2J}(s)=Q_{2T,2J}(s)+\frac{1}{\pi}\int_{(M+\mu)^2}^{\infty}ds'\,\frac{\mathrm{Im}p_{2T,2J}(s')}{s'-s}+\frac{1}{\pi}\int_{0}^{(M-\mu)^2}ds'\,\frac{\mathrm{Im}p_{2T,2J}(s')}{s'-s}+\Delta_J{}^{(T)}(s). \quad (5)$$

In the same manner as before (cf. III for the details) we use crossing symmetry to evaluate $\mathrm{Re}p_{2T,2J}(s)$ and $\mathrm{Im}p_{2T,2J}(s)$ on the crossed cut $0<s\leqslant(M-\mu)^2$. The long-range Born terms $Q_{2T,2J}(s)$ which arise from the pole $s'=M^2$ and the short cut $(M-\mu^2/M)^2\leqslant s'\leqslant(M^2+2\mu^2)$ are readily calculated. In the p-wave case these Born terms are large; this shows that the single nucleon pole and the long range part of the corresponding crossed process give a very important contribution in low energy p-wave $\pi-N$ scattering. The same conclusion was reached by Chew *et al.*[10] using a different method.

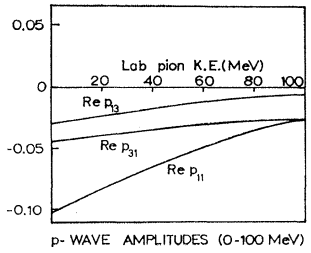

FIG. 7. Values of the small p-wave $\pi-N$ amplitudes $\mathrm{Re}p_{2T,2J}=(\sin 2\alpha_{2T,2J})/2q^3$ where q is the momentum in the c.m. system.

Barnes, Dr. Kinsey, and Dr. Knapp for communicating these results.

[13] Liverpool University result. We are indebted to Dr. Edwards and Dr. Massam for communications about these experiments.

[14] A. Loria *et al.*, Nuovo cimento **22**, 820 (1961).

[15] J. Deahl, M. Derrick, J. Fetkovich, T. Fields, and G. B. Young, Phys. Rev. **124**, 1987 (1961).

[16] This assumption may not be correct. See R. Omnès and G. Valladas, *Proceedings of the Aix-en-Provence International Conference on Elementary Particles* (Centre d'Etudes Nucleaires de Saclay, Seine et Oise, 1961), Vol. I, p. 467.

We shall use the $(\pm)$ charge combinations defined analogously to (1). Our dispersion relations for $p_{2T,2J}(s)$ are now used to evaluate the p-wave discrepancies $\Delta_{1/2}{}^{(\pm)}(s)$ and $\Delta_{3/2}{}^{(\pm)}(s)$ where the subscript is the angular momentum. These discrepancies give the effect of the low-energy $\pi-\pi$ interactions on p-wave $\pi-N$ scattering, coming from the right half of the circle, plus the effect of various short-range interactions (range $\lesssim\hbar/Mc$) coming from the left half of the circle ($|\arg(s')|\geqslant\pi/2$) and the cut $-\infty\leqslant s'\leqslant 0$.

Again we should be able to distinguish the low-energy $\pi-\pi$ parts of $\Delta_{1/2}{}^{(\pm)}(s)$ and $\Delta_{3/2}{}^{(\pm)}(s)$ from the short-range parts by the fact that the former will vary rapidly with s in the range we use ($20\leqslant s\leqslant 32.7$ and $59.6\leqslant s\leqslant 80$), while the short-range parts can be represented by a pole on the cut $-\infty\leqslant s'\leqslant 0$ and contribute to $\Delta_{1/2}{}^{(\pm)}(s)$ and $\Delta_{3/2}{}^{(\pm)}(s)$ a term which varies slowly with s. This separation of the low-energy $\pi-\pi$ effect should be somewhat easier here than in the case of s-wave $\pi-N$ scattering because of the extra factor q^{-2} in the definition of the amplitudes $p_{2T,2J}(s)$. On the left half of the circle and on the cut $-\infty\leqslant s'\leqslant 0$ the factor $|q|^{-2}$ is very small.

The presence of this factor q^{-2} in $p_{2T,2J}(s)$ also makes it much easier to evaluate the dispersion relations for $p_{2T,2J}(s)$. This is because in the physical region $\mathrm{Im}p_{2T,2J}(s)\sim q^{-3}$ as $s\to\infty$ by unitarity, so the physical integral converges faster at high energies than in the s-wave case. Also $q^2\to\infty$ as $s\to 0$, so that the crossed integral is easier to evaluate; uncertainties about the $\pi-N$ phase shifts at the higher energies are not so important as in the s-wave case, and also $\mathrm{Im}p_{2T,2J}(s')\to 0$ as $s'\to 0$. The price we pay for these considerable advantages is that we must know the p-wave $\pi-N$ phase shifts accurately at low energies.

Threshold behavior on the crossed cut. The p-wave $\pi-N$ amplitudes $f_{1-}(s)$ and $f_{1+}(s)$ for angular momentum $J=\frac{1}{2}$ and $J=\frac{3}{2}$, respectively, are expressed in terms of the amplitudes f_1, f_2 (cf. I for notation) by

$$\begin{aligned} f_{1-}(s)&=\tfrac{1}{2}\int_{-1}^{+1}dx[P_1(x)f_1+f_2],\\ f_{1+}(s)&=\tfrac{1}{2}\int_{-1}^{1}dx\,[P_1(x)f_1+P_2(x)f_2], \end{aligned}\tag{6}$$

where $x=\cos\vartheta$ and ϑ is the $\pi-N$ scattering angle in the c.m. system. Also

$$\begin{aligned} f_1&=[(E+M)/8\pi W][A(s,t)+(W-M)B(s,t)],\\ f_2&=[(E-M)/8\pi W][-A(s,t)+(W+M)B(s,t)], \end{aligned}\tag{7}$$

where $E=(M^2+q^2)^{1/2}$ and $W=s^{1/2}$. Applying the crossing relation to the invariant amplitudes $A(s,t)$ and $B(s,t)$ in (7) and substituting in (6), we find $f_{1\pm}(s)$ on the crossed cut $0\leqslant s\leqslant(M-\mu)^2$ in the same way as in III. However, we wish to use the dispersion relation (5) for the amplitudes $p_{2T,2J}$ which are derived from $f_{1\pm}{}^{(T)}(s)$ by dividing by q^2. Also $q^2=0$ at $s=(M-\mu)^2$, so there may be singularities in $p_{2T,2J}(s)$ as $s\to(M-\mu)^2$. We shall now show that the behavior as $s\to(M-\mu)^2$ causes no difficulties.

From (7) we get

$$\begin{aligned} \frac{1}{4\pi}A(s,t)&=\frac{W+M}{E+M}f_1-\frac{W-M}{E-M}f_2,\\ \frac{1}{4\pi}B(s,t)&=\frac{1}{E+M}f_1+\frac{1}{E-M}f_2. \end{aligned}\tag{8}$$

Also, for small physical momentum q'', and physical scattering angle ϑ'',

$$\begin{aligned} f_1&=f_0(q'')+3\cos\vartheta''f_{1+}(q'')+O(q''^4),\\ f_2&=(f_{1-}(q'')-f_{1+}(q''))+O(q''^4), \end{aligned}\tag{9}$$

where f_0, f_{1-}, and f_{1+} denote the s and p-wave $\pi-N$ amplitudes. Using (6) and Eq. (10) of III, we see that for $0<s\leqslant(M-\mu)^2$,

$$\begin{aligned} \pm\mathrm{Re}f_{1-}{}^{(\pm)}(s)=&\frac{(W+M)^2-\mu^2}{32\pi W^2}\int_{-1}^{+1}xdx\\ &\times[\mathrm{Re}A^{(\pm)}(s'',x'')-(W-M)\,\mathrm{Re}B^{(\pm)}(s'',x'')]\\ &+\frac{(W-M)^2-\mu^2}{32\pi W^2}\int_{-1}^{+1}dx\,[-\mathrm{Re}A^{(\pm)}(s'',x'')\\ &-(W+M)\,\mathrm{Re}B^{(\pm)}(s'',x'')], \end{aligned}\tag{10}$$

where the superscripts $(\pm)$ are as usual the charge combinations given by Eq. (1). Also $x''=\cos\vartheta''$. Using (6) a similar equation holds for $\mathrm{Re}f_{1+}{}^{(\pm)}(s)$ for $0<s\leqslant(M-\mu)^2$.

On the crossed cut $0<s\leqslant(M-\mu)^2$, we have

$$s=[(M^2+q^2)^{1/2}-(\mu^2+q^2)^{1/2}]^2,$$

and q^2 increases from 0 as s decreases from $(M-\mu)^2$. Also $x=\cos\vartheta$ is used in defining the partial wave amplitudes on the crossed cut. When s is close to $(M-\mu)^2$, the variables (q^2,x) on the crossed cut are related to the variables (q''^2,x'') in the physical region by [cf. Eqs. (14) and (15) of III]

$$\begin{aligned} q''^2&=q^2\left\{1-\frac{2\mu}{M}(1+x)+O\left(\frac{\mu^2}{M^2}\right)\right\},\\ x''&=x-\frac{2\mu}{M}(1-x^2)+O\left(\frac{\mu^2}{M^2}\right). \end{aligned}\tag{11}$$

The behavior of $\mathrm{Re}\,p_{2T,2J}(s)$. Using (8) and (9) we see that for q'' small,

$$\frac{1}{4\pi}\mathrm{Re}A(s'',x'')=\left(1+\frac{\mu}{2M}\right)a_s - 2M\mu(a_{p\frac{1}{2}}-a_{p\frac{3}{2}})+O(q''^2), \quad (12)$$

$$\frac{1}{4\pi}\mathrm{Re}B(s'',x'')=\frac{1}{2M}a_s+2M(a_{p\frac{1}{2}}-a_{p\frac{3}{2}})+O(q''^2),$$

where a_s, $a_{p\frac{1}{2}}$, and $a_{p\frac{3}{2}}$ are the appropriate s- and p-wave $\pi-N$ scattering lengths. Substituting in (10) we see that because of the factor x in the first integral, this term behaves like q^2 as $q^2\to 0$. The kinematic factor outside the second integral ensures that the second term in (10) has the same behavior. Hence $\mathrm{Re}p_{2T,2J}(s)\to$ const as $s\to(M-\mu)^2$.

The behavior of $\mathrm{Im}p_{2T,2J}(s)$. For $\mathrm{Im}p_{2T,2J}(s)$ the position is not so simple. For example, $\mathrm{Im}f_{1-}{}^{(\pm)}(s)$ is defined by an equation analogous to (10) except for a reversal of signs [Eq. (17) of III]. In the integrals on the right of (10) we now replace $\mathrm{Re}A^{(\pm)}$ and $\mathrm{Re}B^{(\pm)}$ by $\mathrm{Im}A^{(\pm)}$ and $\mathrm{Im}B^{(\pm)}$, respectively. Instead of (12), for small q'' we get

$$\begin{aligned}(1/4\pi)\,\mathrm{Im}A(s'',x'')&=(1+\mu/2M)a_s{}^2q''+O(q''^3),\\ (1/4\pi)\,\mathrm{Im}B(s'',x'')&=(1/2M)a_s{}^2q''+O(q''^3).\end{aligned} \quad (13)$$

Substituting (13) in the analog of Eq. (10) gives

$$\mathrm{Im}p_{2T,2J}(s)=c_{2T,2J}/q+O(q) \quad \text{as} \quad q\to 0, \quad (14)$$

where $c_{2T,2J}$ are constants. [In this case the leading term does not vanish on integration over x, because the relation (11) between q'' and q itself involves x.]

Now consider the crossed integral in the dispersion relation (5) for $\mathrm{Re}p_{2T,2J}(s)$. It is

$$I_{2T,2J}(s)\equiv\frac{1}{\pi}P\int_0^{(M-\mu)^2}ds'\,\frac{\mathrm{Im}p_{2T,2J}(s')}{s'-s}. \quad (15)$$

As $s'\to(M-\mu)^2$,

$$\mathrm{Im}p_{2T,2J}(s')=\{d_{2T,2J}/[(M-\mu)^2-s']^{1/2}\}+O(q'),$$

where $d_{2T,2J}$ are constants. Clearly the integral (15) converges if $s\neq(M-\mu)^2$. Further, by a standard theorem on the limiting behavior of principal value integrals,[17] $I_{2T,2J}(s)$ tends to a finite value as $s\to(M-\mu)^2$. In the actual computation we used an algebraic method to evaluate that part of the crossed integral arising from values of s' close to $(M-\mu)^2$.

Phase Shifts and Errors

The phase shifts used in calculating $\Delta_{1/2}{}^{(\pm)}(s)$ and $\Delta_{3/2}{}^{(\pm)}(s)$ were, with the exception of α_{33}, the accurate values described in Sec. 2(i) above. The values of α_{33} in the range 0 to 500 MeV were given by (i) Woolcock's calculated values for $\mathrm{Re}p_{33}$ from 0 to 100 MeV, (ii) a Chew-Low fit to the experimental values from 80 to 180 MeV, and (iii) a smooth curve drawn through the accurate experimental values above 180 MeV. Assuming complete elasticity, these values gave $\mathrm{Re}p_{33}$ and $\mathrm{Im}p_{33}$ up to 500 MeV. Above 500 MeV the plot of $\mathrm{Im}p_{33}$ was continued smoothly to fit on to a resonance peak at 1.3 BeV, and then to fit on the high-energy behavior $0.22/q^3$ above 2 BeV. From these initial values we calculated

$$\mathrm{Re}p_{33}(s)-\frac{1}{\pi}P\int_{(M+\mu)^2}^{\infty}\frac{\mathrm{Im}p_{33}(s')}{s'-s}ds',$$

and made small adjustments in α_{33} in the neighborhood of the joins of the different ranges so as to smooth out any kinks in this function at the joins. (These small adjustments were within the estimated errors on the initial values of α_{33}.) The final values of α_{33} are shown in Fig. 6; these values were used in our computations of $\Delta_J{}^{(\pm)}(s)$ $(J=\frac{1}{2},\frac{3}{2})$. (The p-wave discrepancies are plotted in Figs. 15 and 22 below.)

The total error in the discrepancies $\Delta_{3/2}{}^{(\pm)}(s)$ arising from errors in the phase shifts α_{11}, α_{13}, α_{31}, α_{33} are estimated to be around ±0.005 for $25\leqslant s\leqslant 32.7$ and $59.6\leqslant s\leqslant 75$. For $75\leqslant s\leqslant 80$ the errors could rise to twice this value, and they may be even larger in $20\leqslant s\leqslant 25$. The total error in $\Delta_{1/2}{}^{(\pm)}(s)$ from the same source are estimated to be about 25% greater than those just quoted for $\Delta_{3/2}{}^{(\pm)}(s)$. The nature of the errors in $\Delta_0{}^{(+)}(s)$ was discussed fully in III. For $\Delta_J{}^{(\pm)}(s)$ $(J=\frac{1}{2},\frac{3}{2})$ we again expect that the shape of the discrepancies is not subject to large errors except for the largest and smallest values of s. The effect of the above errors is mainly to shift the curves $\Delta_J{}^{(\pm)}(s)$ bodily up or down.

In the crossed region there are also errors arising from $\pi-N$ s waves, d waves, etc. For s waves the contributions to the real part and to the crossed integral tend to cancel, and the errors arising from α_1 and α_3 are estimated to be small. Below 400 MeV the d-wave phase shifts are small and the d-wave contribution is only noticeable (in the real parts) for $s<25$ (it comes from δ_{13}). Apart from the region $20\leqslant s<25$ errors due to uncertainties in the d waves are negligible. The above estimates of the p-wave errors in $\Delta_J{}^{(\pm)}(s)$ $(J=\frac{1}{2},\frac{3}{2})$ are therefore believed to be good estimates of the total errors in $\Delta_J{}^{(\pm)}(s)$.

Errors near the thresholds. It will be seen below that the values of $\Delta_J{}^{(\pm)}(s)$ $(J=\frac{1}{2},\frac{3}{2})$ near the thresholds $s=(M\pm\mu)^2$ are of particular interest, and we examine the errors in these regions in more detail. The contributions to $\Delta_J{}^{(\pm)}(s)$ from the s-wave phase shifts α_1 and α_3 show the sort of cancellation mentioned in the preceding paragraph, and thus the main contribution to errors in the shape of $\Delta_J{}^{(\pm)}(s)$ near the thresholds

[17] See for example, J. Hamilton and W. S. Woolcock, reference 9, Sec. 2(ii) for details.

comes from the p-wave phase shifts. The errors are only important in $\mathrm{Re}p_{2T,2J}(s)$ and their size can be seen from the errors given by Woolcock[9] for his p-wave scattering lengths ($\hbar=\mu=c=1$):

$$\begin{aligned} a_{33} &= \ 0.214\pm0.004, \\ a_{11} &= -0.104\pm0.006, \\ a_{31} &= -0.040\pm0.004, \\ a_{13} &= -0.030\pm0.005. \end{aligned} \tag{16}$$

We shall discuss in Sec. 3(xii) below the extent to which some of our deductions depend on (16) giving a realistic estimate of the errors in the p-wave scattering lengths.

3. THE $T=0$ π–π INTERACTION

In the preceding sections we found the experimental values of the discrepancies $\Delta_0^{(+)}(s)$, $\Delta_{1/2}^{(+)}(s)$, and $\Delta_{3/2}^{(+)}(s)$ for the s, $p_{1/2}$, and $p_{3/2}$ partial wave $\pi-N$ amplitudes, respectively. Now we try to find the low energy $\pi-\pi$ interaction in the $T=0$ isotopic state which reproduces these discrepancies. In each case we can add to the $\pi-\pi$ contribution a slowly varying function of s which represents the short range part of the $\pi-N$ interaction, as discussed in Sec. 2(i) above. We also attempt to assess how unique is our result for the low-energy $T=0$ $\pi-\pi$ interaction.

(i) Absorptive Parts on the Circle $|s|=M^2-\mu^2$

The absorptive parts of the amplitudes $A^{(\pm)}(s,t)$, $B^{(\pm)}(s,t)$ in the channel $\pi+\pi\to N+\bar{N}$ are given by[18]

$$\begin{aligned} &\mathrm{Im}A_{\pi\pi}^{(\pm)}(s,t) \\ &=\frac{8\pi}{p_-^2}\sum_{J=0}^{\infty}(J+\tfrac{1}{2})(ip_-q_3)^J\Big[P_J(\cos\vartheta_3)\,\mathrm{Im}f_+^J(t) \\ &\quad-\frac{M}{[J(J+1)]^{1/2}}\cos\vartheta_3 P_J'(\cos\vartheta_3)\,\mathrm{Im}f_-^J(t)\Big], \end{aligned} \tag{17}$$

$$\begin{aligned} &\mathrm{Im}B_{\pi\pi}^{(\pm)}(s,t) \\ &=8\pi\sum_{J=1}^{\infty}\frac{(J+\frac{1}{2})}{[J(J+1)]^{1/2}}(ip_-q_3)^{J-1}P_J'(\cos\vartheta_3)\,\mathrm{Im}f_-^J(t). \end{aligned}$$

Here q_3 and ip_- are the pion and nucleon momenta (in the c.m. system) in the channel $\pi+\pi\to N+\bar{N}$. They are given by

$$q_3^2=t/4-\mu^2, \quad p_-^2=M^2-t/4. \tag{18}$$

Also

$$\cos\vartheta_3=(s-p_-^2+q_3^2)/(2ip_-q_3) \tag{19}$$

gives the scattering angle ϑ_3 in the channel $\pi+\pi\to N+\bar{N}$. Further, $f_\pm^J(t)$ are the helicity amplitudes for $\pi+\pi\to N+\bar{N}$ (for states having total angular momentum J) as defined by Jacob and Wick.[19] In finding the discontinuity of a $\pi-N$ partial wave amplitude across the circle $|s|=M^2-\mu^2$ we use[20] (17) with $t\geqslant 4\mu^2$. Frazer and Fulco[18] have shown that the Legendre expansions in (17) converge only for that part of the circle given by $|\arg s|\lesssim 66°$. We shall, throughout, only calculate the circle contribution coming from this arc; this will include all the long-range effects of the $\pi-\pi$ interaction on $\pi-N$ scattering. The contribution to $\Delta^{(+)}(s)$ from the remainder of the circle ($66°<|\arg s|<180°$) is assumed to be included in the short-range part of the $\pi-N$ interaction. In the charge combinations given by the superscripts $(+)$ and $(-)$ only even and odd values of J, respectively, appear on the right of (17). Also $f_-^0(t)=0$.

(ii) Symmetry Properties of $\Delta^{(+)}(s)$ if the $J=0$ π–π Interaction only Contributes

Now we consider the $(+)$ case and assume that we can ignore any low-energy $\pi-\pi$ interactions in states with angular momentum $J\geqslant 2$. Then by (17)

$$\begin{aligned} &\mathrm{Im}A_{\pi\pi}^{(+)}(s,t)=[4\pi/(M^2-t/4)]\,\mathrm{Im}f_+^0(t), \\ &\mathrm{Im}B_{\pi\pi}^{(+)}(s,t)=0. \end{aligned} \tag{20}$$

The contribution of this $J=0$ $\pi-\pi$ interaction to the scattering process $\pi+N\to\pi+N$ at energy s and c.m. angle ϑ is given by[21]

$$\begin{aligned} A_{\pi\pi}^{(+)}(s,\cos\vartheta)&=\frac{1}{\pi}\int_{t'=4\mu^2}^{\infty}\frac{\mathrm{Im}A_{\pi\pi}^{(+)}(s,t')}{t'+2q^2(1-\cos\vartheta)}dt', \\ B_{\pi\pi}^{(+)}(s,\cos\vartheta)&=0, \end{aligned} \tag{21}$$

where q is the c.m. momentum in the channel $\pi+N\to\pi+N$.

It is now easy to find the $T=0$, $\pi-\pi$ contribution to any $\pi-N$ partial wave amplitude. For example consider the p-wave amplitudes $f_{1/2}^{(+)}(s)$ and $f_{3/2}^{(+)}(s)$ where the subscript is the angular momentum. [When divided by q^2 these give the amplitudes $p_{2T,2J}(s)$ used in Sec. 2(ii) above.] Using Eqs. (10) and (21) the $T=0$ $\pi-\pi$ contribution is

$$\begin{aligned} &[\mathrm{Re}f_{1/2}^{(+)}(s)]_{\pi\pi} \\ &=\frac{(W+M)^2-\mu^2}{32\pi W^2}\int_{-1}^{+1}dx\,xA_{\pi\pi}^{(+)}(s,x) \\ &\quad-\frac{(W-M)^2-\mu^2}{32\pi W^2}\int_{-1}^{+1}dx\,P_0(x)A_{\pi\pi}^{(+)}(s,x), \end{aligned} \tag{22}$$

[18] See W. R. Frazer and J. R. Fulco, Phys. Rev. **119**, 1420 (1960).

[19] M. Jacob and G. C. Wick, Ann. Phys. (New York) **7**, 404 (1959).

[20] See I and III for the details of this relation.

[21] See III, Eqs. (45) and (46).

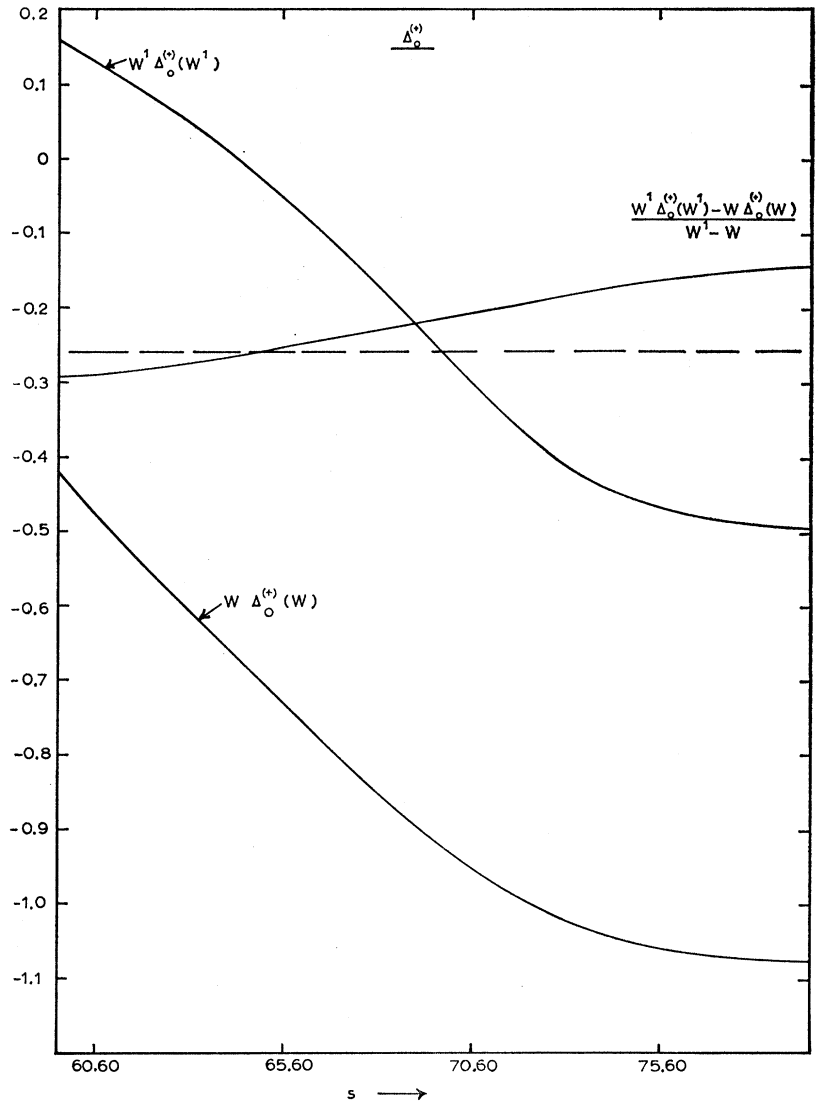

FIG. 8. Test of Lovelace's relation for the s-wave $\pi-N$ discrepancy $\Delta_0^{(+)}(s)$.

$$[\mathrm{Re}f_{3/2}^{(+)}(s)]_{\pi\pi}$$
$$=\frac{(W+M)^2-\mu^2}{32\pi W^2}\int_{-1}^{+1}dx\,xA_{\pi\pi}^{(+)}(s,x)$$
$$-\frac{(W-M)^2-\mu^2}{32\pi W^2}\int_{-1}^{+1}dx\,P_2(x)A_{\pi\pi}^{(+)}(s,x), \quad (23)$$

where $x\equiv\cos\vartheta$ and $W\equiv s^{1/2}$. By (20) and (21) $A_{\pi\pi}^{(+)}(s,x)$ is a function of q^2 and x only (i.e., s does not appear explicitly in this special case). Now to each positive value of q^2 correspond two values of W given by

$$W=(M^2+q^2)^{1/2}+(\mu^2+q^2)^{1/2},$$
$$W'=(M^2+q^2)^{1/2}-(\mu^2+q^2)^{1/2}, \quad (24)$$

where we take the positive value of the square roots. W lies on the physical cut $s\geqslant(M+\mu)^2$ and W' lies on the crossed cut $0\leqslant s\leqslant(M-\mu)^2$, and they are related by

$$WW'=M^2-\mu^2. \quad (25)$$

The kinematic factors appearing outside the integrals in (22) and (23) can be written

$$\frac{(W\pm M)^2-\mu^2}{W^2}=\frac{1}{W}\left(W+\frac{M^2-\mu^2}{W}\pm 2M\right). \quad (26)$$

Apart from the common factor W^{-1}, these expressions on the right of (26) are unaltered if we replace W by W'. Hence, using the subscript $\pi\pi$ to denote the $J=0$ $\pi-\pi$ contribution to the p-wave discrepancies $\Delta^{(+)}(s)$ $(j=\frac{1}{2},\frac{3}{2})$, we have

$$W\Delta_{1/2,\pi\pi}^{(+)}(W)=W'\Delta_{1/2,\pi\pi}^{(+)}(W'), \quad (27)$$
$$W\Delta_{3/2,\pi\pi}^{(+)}(W)=W'\Delta_{3/2,\pi\pi}^{(+)}(W'). \quad (28)$$

Similarly it is obvious that for the s-wave discrepancy,

$$W\Delta_{0,\pi\pi}{}^{(+)}(W)=W'\Delta_{0,\pi\pi}{}^{(+)}(W'). \tag{29}$$

In this proof it has been assumed that the integration over t' in (21) extends over all values greater than $4\mu^2$. In the actual calculations (as was pointed out above) we confine the integration over the $\pi+\pi\to N+\bar{N}$ channel to the front part of the circle given by $|\arg s|\leqslant 66°$. This procedure is equivalent to replacing the upper limit of integration in (21) by $t'=\frac{1}{2}(1-x)t_{\max}$, where[22] $t_{\max}=4[\mu^2\cos^2(33°)+M^2\sin^2(33°)]$. Clearly the symmetry relations (27), (28), and (29) are still valid; the subscript $\pi\pi$ now indicates that part of the discrepancy which is due to the $J=0$ $\pi-\pi$ interaction and comes from the front of the circle, $|\arg s|\leqslant 66°$. We are much indebted to Dr. Lovelace for pointing[23] out the existence of these relations (27), (28), and (29).

(iii) Test of Lovelace's Relations

A. s-wave Discrepancy

We now examine how well these symmetry relations (27), (28), and (29) are satisfied. Consider first the s-wave $\pi-N$ results, and use the values of $\Delta_0{}^{(+)}(s)$ shown in Fig. 2. Let

$$\Delta_0{}^{(+)}(W)=\Delta_{0,\pi\pi}{}^{(+)}(W)+F_0(W), \tag{30}$$

where $\Delta_{0,\pi\pi}{}^{(+)}(W)$ is the long-range contribution from the $J=0$ $\pi-\pi$ interaction as defined above and $F_0(W)$ is the remainder (it comes from short-range effects associated with the cut $-\infty\leqslant s\leqslant 0$, and with the left-hand part of the circle: $|\arg s|>66°$; it might also include some long-range effect from any low-energy $J=2$ $\pi-\pi$ interaction which contributes to the front of the circle). By (29),

$$\frac{W'\Delta_0{}^{(+)}(W')-W\Delta_0{}^{(+)}(W)}{W'-W}=\frac{W'F_0(W')-WF_0(W)}{W'-W}. \tag{31}$$

Suppose $F_0(W)$ is due entirely to short-range effects. Then to a fair approximation we can represent these by

$$F_0(W)=-\alpha-\beta/W^2 \tag{32}$$

where α, β are constants. Also, the general discussion of the form of $\Delta_0{}^{(+)}(s)$ given in II and III suggests that both α and β are positive. With this form for $F_0(W)$ the right-hand side of (31) becomes $-\alpha+\beta(M^2-\mu^2)^{-1}$ so it is independent of W. We plot the left-hand side of (31) in Fig. 8. The variation of this function with W is seen to be small. This fact is further confirmation of our general assertion that the rapidly varying part of $\Delta_0{}^{(+)}(s)$ in the regions $20\leqslant s\leqslant 32.7$ and $59.6\leqslant s\leqslant 80$ is almost entirely due to a low-energy $J=0$ $\pi-\pi$ interaction.

[22] See Eqs. (3) and (4) of III.
[23] C. Lovelace (private communication).

Possible evidence for $J=2$ $\pi-\pi$ interaction. The function $[W'\Delta_0{}^{(+)}(W')-W\Delta_0{}^{(+)}(W)]/(W'-W)$ shown in Fig. 8 is not a constant, but varies slowly with W. This could be due either to the fact that (32) is not a good approximation to the short range part of the discrepancy, or to the presence of some $J=2$ $\pi-\pi$ contribution. If we use the somewhat better form

$$F_0(W)=-\alpha-\beta/(W^2+W_0{}^2) \tag{33}$$

(where α, β, and $W_0{}^2$ are positive constants) for the short-range part, we can readily evaluate the right side of (31). Although the use of (33) could possibly give the full variation with W shown in Fig. 8, it seems more likely that a small effect due to $J=2$ $\pi-\pi$ scattering is present.

B. p-wave Discrepancies

The values of

$$[W'\Delta_j{}^{(+)}(W')-W\Delta_j{}^{(+)}(W)]/(W'-W),\quad (j=\tfrac{1}{2},\tfrac{3}{2}),$$

are shown in Fig. 9. Apart from the small kinks for $59.6\leqslant s\leqslant 65$, the curves are very smooth and slowly varying functions of W. (The small kinks may well be due to small errors in the $\pi-N$ data near threshold.)

This again is consistent with our general picture, namely, that the rapidly varying parts of the p-wave discrepancies $\Delta_j{}^{(+)}(s)$ $(j=\frac{1}{2},\frac{3}{2})$ are due to the effect of the low-energy $J=0$ $\pi-\pi$ interaction. In this case the presence of the extra factor q^{-2} in the amplitudes $[p_{2T,2J}(s)]$ means that the contribution to $\Delta_j{}^{(+)}(s)$ from the very front of the circle (i.e., near $s=M^2-\mu^2$) is enhanced relative to other contributions. This is because the factor $|q|^{-2}$ is small on all parts of the cuts which are far away from the thresholds $s=(M\pm\mu)^2$ (cf. Fig. 1), so the contributions from these parts of the cuts are suppressed in the dispersion relations (5) for $p_{2T,2J}(s)$. This tends to make the discrepancies $\Delta_{1/2}{}^{(+)}(s)$ and $\Delta_{3/2}{}^{(+)}(s)$ themselves obey (27) and (28).

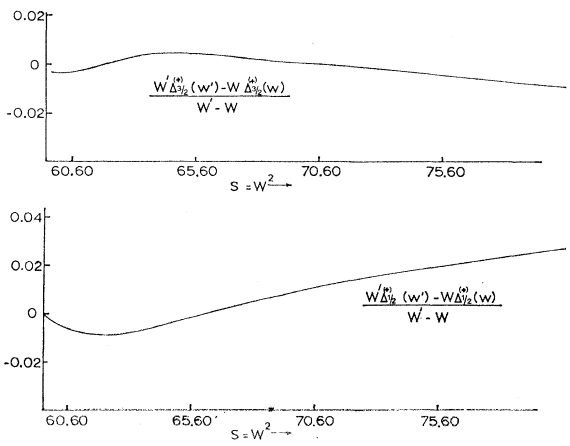

FIG. 9. Test of Lovelace's relation for the p-wave $\pi-N$ discrepancies $\Delta_{1/2}{}^{(+)}(s)$ and $\Delta_{3/2}{}^{(+)}(s)$.

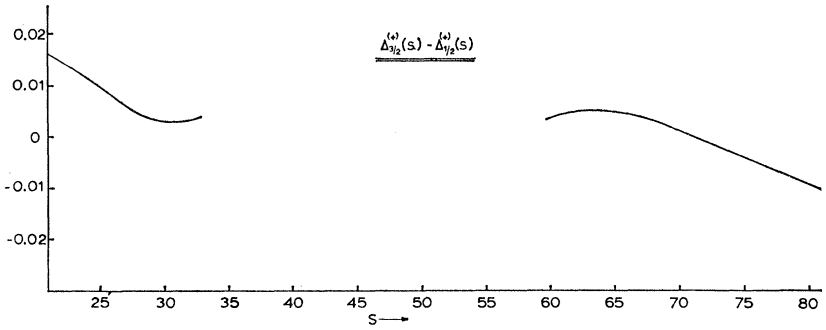

FIG. 10. The difference of the p-wave $\pi-N$ discrepancies $[\Delta_{3/2}^{(+)}(s)-\Delta_{1/2}^{(+)}(s)]$.

(iv) The Difference $[\mathbf{\Delta}_{\frac{3}{2}}^{(+)}(s)-\mathbf{\Delta}_{\frac{1}{2}}^{(+)}(s)]$

It is readily seen from (6), (17), and (20) that if the low-energy $T=0$ $\pi-\pi$ interaction is negligible in the states $J\geqslant 2$, then

$$[\Delta_{3/2,\pi\pi}^{(+)}(s)-\Delta_{1/2,\pi\pi}^{(+)}(s)]/\tfrac{1}{2}[\Delta_{3/2,\pi\pi}^{(+)}(s)+\Delta_{1/2,\pi\pi}^{(+)}(s)]=O(t'/M^2). \quad (34)$$

Here t' is a weighted average of the value of t for which the contribution from the $T=0$, $J=0$ $\pi-\pi$ interaction to low-energy $\pi-N$ scattering is important. We estimate $t'\simeq 10\mu^2-15\mu^2$. Thus Eq. (34) suggests that $[\Delta_{3/2}^{(+)}(s)-\Delta_{1/2}^{(+)}(s)]$ is predominantly due to short-range effects. The experimental values of this quantity are shown in Fig. 10. The general behavior is a slow falling off as s increases from 20 to 80. The small deviations from a monotonically decreasing function of s could be due to small $T=0$, $J=2$ $\pi-\pi$ effects, and to the fact that the right-hand side of (34) is not actually zero. However the general behavior of $\Delta_{3/2}^{(+)}(s)-\Delta_{1/2}^{(+)}(s)$ over the wide range $20\leqslant s\leqslant 80$ is further confirmation that the main effect which we are detecting in the (+) case is the $T=0$, $J=0$ $\pi-\pi$ interaction.

(v) Determination of $\mathrm{Im}f_+^0(t)$ from the Discrepancies

Suppose now that we can isolate the $\pi-\pi$ parts of the $\Delta^{(+)}$ discrepancies in the ranges $20\leqslant s\leqslant 32.7$ and $59.6\leqslant s\leqslant 80$. Denote them by $\Delta_{0,\pi\pi}^{(+)}(s)$, $\Delta_{j,\pi\pi}^{(+)}(s)$ $(j=\frac{1}{2},\frac{3}{2})$ and ignore any $J=2$ $\pi-\pi$ contribution to the discrepancies. We shall examine the kind of information which this gives us about the absorptive part of the helicity amplitude $\mathrm{Im}f_+^0(t)$ for $t\geqslant 4\mu^2$.

Using (17), (22), (23), and the analogous equation for the s-wave case, we can write

$$\Delta_{0,\pi\pi}^{(+)}(s)=\int_{4\mu^2}^{56\mu^2}K_0^{(+)}(s,t)\,\mathrm{Im}f_+^0(t)dt, \quad (35)$$

$$\Delta_{j,\pi\pi}^{(+)}(s)=\int_{4\mu^2}^{56\mu^2}K_j^{(+)}(s,t)\,\mathrm{Im}f_+^0(t)dt, \quad (j=\tfrac{1}{2},\tfrac{3}{2}) \quad (36)$$

where we have cut off the integration at $t=56\mu^2$.[24] The kernels $K_0^{(+)}(s,t)$, $K_j^{(+)}(s,t)$ are fairly complicated functions of various kinematic factors. The values of these functions for the s-wave and $p_{3/2}$-wave $(j=\frac{3}{2})$ cases are shown in Figs. 11 and 12 for various values of s. The form of $K_{1/2}^{(+)}(s,t)$ is almost the same as $K_{3/2}^{(+)}(s,t)$. (The relative scales of $K_j^{(+)}$ and $K_0^{(+)}$ are unimportant.)

We note the following general properties of the kernels.

(i) For different fixed values of s, the kernel $K^{(+)}(s,t)$ gives functions of t (some of them are shown in Fig. 11). Over the range $8\mu^2\leqslant t\leqslant 30\mu^2$ these are almost geometrically similar functions[25] of t. This is true except for s near the extreme values ($s=20$ and $s=80$). The kernels $K_j^{(+)}(s,t)$ $(j=\frac{1}{2},\frac{3}{2})$ tend to have the same property, but not to such a marked extent.

(ii) In the kernels $K_j^{(+)}(s,t)$ $(j=\frac{1}{2},\frac{3}{2})$ small values of t $(4\mu^2\leqslant t\leqslant 15\mu^2)$ are much more important than the larger values of t $(t>15\mu^2)$. This effect is much less marked in $K_0^+(s,t)$.

(iii) In general, the kernels are larger for the crossed cut $(s\leqslant 32.7)$ than for the physical cut $(s\geqslant 59.6)$.

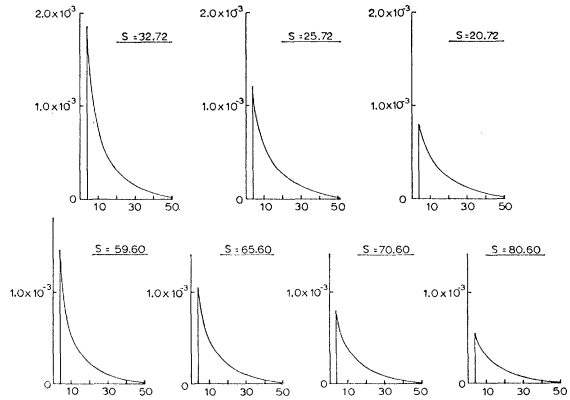

FIG. 11. Examples, for various values of s, of the kernels $K_0^{(+)}(s,t)$ which relate the helicity amplitude $f_+^0(t)$ to the $\pi-\pi$ part of the discrepancy for s-wave $\pi-N$ scattering [Eq. (35)].

[24] The largest value of t which can contribute to the arc of the circle $|\mathrm{arg}s|\leqslant 66°$ is $56\mu^2$.

[25] By this we mean that if, for different fixed values of s, we multiply the functions $K_1^{(+)}(s,t)$ by constants so as to make them equal for $t=15\mu^2$, say, they will then be almost equal over the range $8\mu^2\leqslant t\leqslant 30\mu^2$.

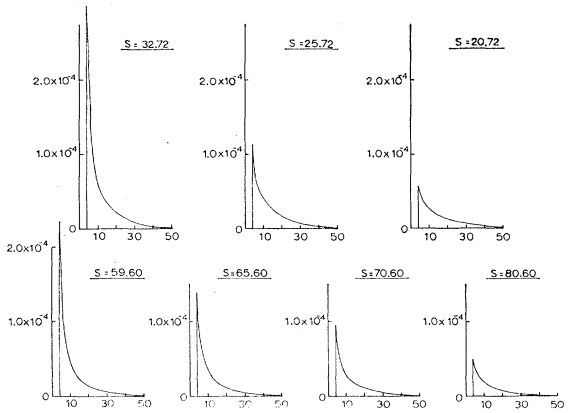

FIG. 12. Examples, for various values of s, of the kernels $K_{3/2}^{(+)}(s,t)$ which relate the helicity amplitude $f_+^0(t)$ to the $\pi-\pi$ part of the $J=\frac{3}{2}$ p-wave discrepancy [Eq. (36)].

We draw the following conclusions:

(a) [from (i)] The *shape*[26] of the function $\Delta_{0,\pi\pi}{}^{(+)}(s)$ is, to a first approximation, independent of the values we choose for $\mathrm{Im}f_+^0(t)$, particularly if we ignore values of s close to the extremes ($s=20$ and $s=80$). Combined with the fact that we can choose values of $\mathrm{Im}f_+^0(t)$ which give good agreement with our experimental values of $\Delta_0^{(+)}(s)$ [cf. Secs. 3(viii) and 3(x) below], this provides further strong confirmation that we are here detecting the $T=0$, $J=0$ $\pi-\pi$ effect[27] in $\pi-N$ scattering. Conversely, it is clear that $\Delta_0^{(+)}(s)$, to a first approximation, only determines one "moment" of $\mathrm{Im}f_+^0(t)$ (this is given, for example, by (35) with $s=59.6$).

(b) [from (i) and (ii)] The experimental values of $\Delta_j^{(+)}(s)$ ($j=\frac{1}{2},\frac{3}{2}$) give us "moments" of $\mathrm{Im}f_+^0(t)$ which are heavily weighted for the smaller values of t. Hence, the p-wave discrepancies are strongly influenced by any low energy $J=0$ $\pi-\pi$ scattering.

(c) [from (iii)] The $\pi-\pi$ effect for $s\leqslant 32.7$ is in all cases stronger than the $\pi-\pi$ effect for $s\geqslant 59.6$. Also, the $\pi-\pi$ effect falls off with decreasing s ($s\leqslant 32.7$) in a manner which cannot be confused with a short-range term (cf. Figs. 2, 15, and 19). Therefore good and unambiguous evidence about the "moments" of $\mathrm{Im}f_+^0(t)$ [as given by (35) and (36)] should be obtained by fitting the discrepancies in the crossed region, $s\leqslant 32.7$ as well as in the physical region, $s\geqslant 59.6$.

(vi) Calculation of $\mathrm{Im}f_+^0(t)$ in Terms of the $J=0$ $\pi-\pi$ Interaction

We now discuss how the quantity $\mathrm{Im}f_+^0(t)$ is calculated for $t\geqslant 4\mu^2$, assuming certain simple forms for the $J=0$, $T=0$ $\pi-\pi$ phase shift $\delta_0^0(t)$. We shall require that the calculated function $\mathrm{Im}f_+^0(t)$ gives the observed $\pi-\pi$ part of the discrepancies.

[26] We use the word in the sense that $\lambda h(s)$ has the same shape as $h(s)$, where λ is a constant.

[27] A low-energy $T=0$, $J=2$ $\pi-\pi$ interaction would give $\Delta_0^{(+)}(s)$ a different shape.

The helicity amplitude $f_+^0(t)$ for the process $\pi+\pi\to N+\bar{N}$ has cuts[28] along $-\infty\leqslant t\leqslant a$ and $4\mu^2\leqslant t\leqslant\infty$, where $a=4\mu^2(1-\mu^2/4M^2)$. The value of $\mathrm{Im}f_+^0(t)$ on $0\leqslant t\leqslant a$ is given by the Born term alone, and is readily calculated using $f^2=0.081$ for the $\pi-N$ coupling constant.[29] For $-25\mu^2\leqslant t\leqslant 0$ we also have contributions to $\mathrm{Im}f_+^0(t)$ from the $\pi-N$ partial wave amplitudes.[28] It is sufficient for the purpose of the present work to use the $(\frac{3}{2},\frac{3}{2})$ amplitude alone. [The small p-wave $\pi-N$ amplitudes give a negligible contribution. The s-wave $\pi-N$ amplitudes give rise to an integrable divergence in $[\mathrm{Im}f_+^0(t)]$[11] at $t=0$, but this gives no trouble in the dispersion relation for the helicity amplitude, Eq. (52) below. In fact, it turns out that the s-wave contribution to $\mathrm{Im}f_+^0(t)$ is negligible. Also, the $\pi-N$ d-wave terms are unimportant for $t>-25\mu^2$.]

We find that the $(\frac{3}{2},\frac{3}{2})$ $\pi-N$ amplitude gives a contribution to $\mathrm{Im}f_+^0(t)$ which increases like $|t|$ when t takes large negative values. For $t<-25\mu^2$ the partial wave expansion for $\mathrm{Im}f_+^0(t)$ in terms of the $\pi-N$ amplitudes is expected to diverge[28] and we cannot reliably determine $\mathrm{Im}f_+^0(t)$ in this region. Figure 13 shows $\mathrm{Im}f_+^0(t)$ for $t\leqslant a$.

By unitarity, $f_+^0(t)$ has the phase $\exp[i\delta_0^0(t)]$ when $4\mu^2\leqslant t\leqslant 16\mu^2$. We assume that, because of the small phase space available for 4π states, this unitarity relation is also approximately true when t lies somewhat above $16\mu^2$, say for $t\leqslant 30\mu^2$. Ignoring further inelastic contributions on the remainder of the right-hand cut we solve for $\mathrm{Im}f_+^0(t)$ in the usual way,[30] assuming $\delta_0^0(t)$ is known for $t\geqslant 4\mu^2$. Because of the approximate nature of the unitary condition for $16\mu^2\leqslant t\leqslant 30\mu^2$, and because of neglecting inelastic contributions on the cut $t\geqslant 30\mu^2$, there will be errors[31] in our values of $\mathrm{Im}f_+^0(t)$ for the larger values of t (say, $20\mu^2\leqslant t\leqslant 56\mu^2$). However the kernels $K^{(+)}(s,t)$ (Figs. 11, 12) are small when t is large, so that these errors are unimportant in calculating the discrepancies.

(vii) The N/D Pole Method

We use the N/D method to give a convenient parametric description of the $T=0$, $J=0$ $\pi-\pi$ phase shift $\delta_0^0(t)$ at low energies. The invariant form of the $T=0$, $J=0$ $\pi-\pi$ partial wave amplitude is

$$A(\nu)=\left(\frac{\nu+1}{\nu}\right)^{1/2}e^{i\delta_0^0}\sin\delta_0^0, \tag{37}$$

[28] Compare with W. R. Frazer and J. R. Fulco, Phys. Rev. **117**, 1603 (1960).

[29] W. S. Woolcock, *Proceedings of the Aix-en-Provence International Conference on Elementary Particles* (Centre d'Etudes Nucleaires de Saclay, Seine et Oise, 1961), Vol. I, p. 459.

[30] R. Omnès, Nuovo cimento **8**, 316 (1958); and W. R. Frazer and J. R. Fulco reference 28.

[31] Several authors [J. S. Ball and D. Y. Wong, Phys. Rev. Letters **7**, 390 (1961); M. Jacob, G. Mahoux and R. Omnès, Nuovo cimento **23**, 838 (1962)] have suggested that the inelastic contributions do not produce large errors.

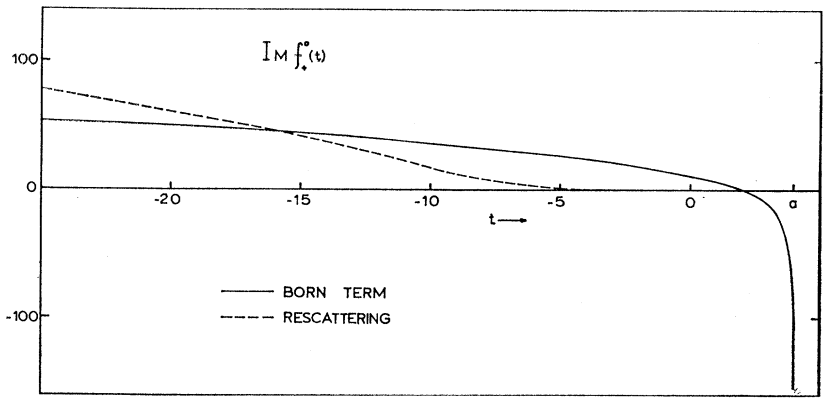

FIG. 13. The value of $\mathrm{Im}f_+^0(t)$ for $-25\leqslant t\leqslant a$. The Born and rescattering terms are to be added.

where δ_0^0 is real in the elastic region; $\nu=q_3^2$, where q_3 is the pion momentum in the c.m. system, and $\mu=1$. $A(\nu)$ has cuts along $-\infty\leqslant\nu\leqslant-1$ and $0\leqslant\nu\leqslant\infty$, and we can write

$$A(\nu)=N(\nu)/D(\nu). \tag{38}$$

The only singularities of $N(\nu)$ and $D(\nu)$ are cuts along $-\infty\leqslant\nu\leqslant-1$ and $0\leqslant\nu\leqslant\infty$, respectively.

It is easy to see that[32]

$$\begin{aligned}\mathrm{Im}N(\nu)&=D(\nu)\,\mathrm{Im}A(\nu), &\nu\leqslant-1\\ &=0, &\nu>-1\end{aligned} \tag{39}$$

and

$$\begin{aligned}\mathrm{Im}D(\nu)&=-N(\nu)R\left(\frac{\nu}{\nu+1}\right)^{1/2}, &\nu\geqslant0\\ &=0, &\nu<0\end{aligned} \tag{40}$$

where R is the ratio of the total to the elastic cross section for $\pi+\pi$ in the $T=0$, $J=0$ state. Putting $R=1$ and using one subtraction at $\nu=\nu_0$, Eq. (40) gives

$$D(\nu)=1-\frac{\nu-\nu_0}{\pi}\int_0^\infty d\nu'\left(\frac{\nu'}{\nu'+1}\right)^{1/2}\frac{N(\nu')}{(\nu'-\nu_0)(\nu'-\nu)}, \tag{41}$$

where we have chosen $D(\nu_0)=1$. On $0\leqslant\nu\leqslant3$, $D(\nu)$ has the phase[33] $\exp[-i\delta_0^0(\nu)]$, so $D(\nu)f_+^0(t)$ is real on this segment of the real axis [note that $t=4(\nu+1)$]. Writing $g(t)=D(\nu)f_+^0(t)$, we have for $t\geqslant4$ the approximate solution for $f_+^0(t)$ (if no subtraction is necessary),

$$g(t)=\frac{1}{\pi}\int_{-\infty}^{a}dt'\frac{\mathrm{Im}g(t')}{t'-t}. \tag{42}$$

Thus for $t\geqslant4$

$$f_+^0(t)=\frac{1}{\pi D(\nu)}\int_{-\infty}^{a}dt'\frac{D(\nu')\,\mathrm{Im}f_+^0(t')}{t'-t}. \tag{43}$$

[32] See G. F. Chew, in *Dispersion Relations*, edited by G. R. Screaton (Oliver & Boyd, Edinburgh, 1961).

[33] As discussed above, we assume also that this is approximately true when $3\leqslant\nu\lesssim6$.

The Effective-Range Formula and the Behavior of the $\pi-\pi$ Solutions

In the spirit of the effective range formula we replace the discontinuity in $\mathrm{Im}A(\nu')$ for $-\infty\leqslant\nu'\leqslant-1$ by a δ function at $\nu=\nu_1$ where ν_1 is negative. Thus

$$\mathrm{Im}A(\nu')=-\pi\Gamma\delta(\nu-\nu_1), \tag{44}$$

where Γ is a constant. By (39) this gives

$$N(\nu)=D(\nu_1)\Gamma/(\nu-\nu_1).$$

We can choose $\nu_0=\nu_1$ so $D(\nu_1)=1$, and

$$N(\nu)=\Gamma/(\nu-\nu_1). \tag{45}$$

The two real parameters ν_1 and Γ determine the phase shift $\delta_0^0(t)$. Substituting (45) in (41) gives

$$D(\nu)=1-\frac{\Gamma}{\pi}(\nu-\nu_1)\int_0^\infty d\nu'\times\left(\frac{\nu'}{\nu'+1}\right)^{1/2}\frac{1}{(\nu'-\nu_1)^2(\nu'-\nu)}. \tag{46}$$

As $\nu_1<0$, the factor $(\nu'-\nu_1)^2$ in the denominator gives no trouble. The explicit form of $D(\nu)$ is given in Appendix I. We have

$$\mathrm{Re}D(\nu)=1+\frac{\Gamma}{\pi}\left(\frac{F(\nu)-F(\nu_1)}{\nu-\nu_1}-F'(\nu_1)\right), \tag{47}$$

where the real (and positive) function $F(\nu)$ is given in Appendix I. Equation (47) is true for all real ν and for any[34] $\nu_1<0$.

Positive values of Γ correspond to an attractive equivalent potential for the $T=0$, $J=0$ $\pi-\pi$ system. The relation of the phase shift δ_0^0 given by (37) and (38) to the usual effective-range formula,

$$\left(\frac{\nu}{\nu+1}\right)^{1/2}\cot\delta_0^0=\frac{1}{a_0}+\frac{1}{2}r\nu+\cdots, \tag{48}$$

[34] Solutions obtained using (44) and (45) with ν_1 in the range $-1<\nu_1<0$ turn out not to give satisfactory agreement with our discrepancies [Sec. 3 (ix) below].

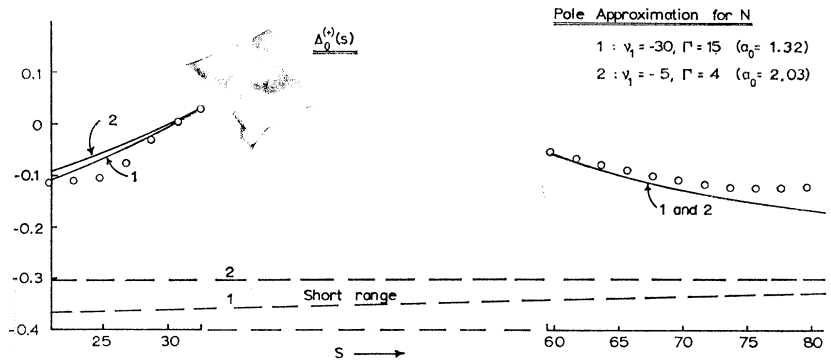

FIG. 14. The N/D pole approximation fits to the s-wave discrepancy $\Delta_0^{(+)}(s)$ are given by the solid lines. The corresponding short range parts are given by the broken lines. The circles indicate the experimental values calculated in Sec. 2.

is given by

$$\frac{1}{a_0}=\frac{(-\nu_1)}{\Gamma}-\frac{1}{\pi}[F(\nu_1)-\nu_1F'(\nu_1)],$$
$$\frac{1}{2}r=\frac{2}{\pi}+\frac{1}{\Gamma}-\frac{1}{\pi}F'(\nu_1). \tag{49}$$

Also, $F(\nu_1)-\nu_1F'(\nu_1)>0$ (for $\nu_1<0$), and a bound state of the $\pi-\pi$ system appears when Γ has increased to a critical value given by

$$\pi/\Gamma_{\text{crit}}=F(\nu_1)/(-\nu_1)+F'(\nu_1). \tag{50}$$

It follows from the properties of $F(\nu)$ given in Appendix I that for $\Gamma>\Gamma_{\text{crit}}$, $D(\nu)$ has one zero on the negative axis at ν_2 where $\nu_1<\nu_2<0$. In this case $\text{Re}D(\nu)$ also vanishes on the real axis at $\nu=\nu_3>0$, so at $\nu=\nu_3$, $\cot\delta_0^0=0$. Also, for $0<\nu<\nu_3$, $\cot\delta_0^0<0$ and for $\nu_3<\nu<\infty$, $\cot\delta_0^0>0$. It is therefore convenient to use the convention, which would follow from Levinson's theorem, that for $\Gamma>\Gamma_{\text{crit}}$, $\delta_0^0=\pi$ when $\nu=0$ and δ_0^0 *decreases* through $\pi/2$ at $\nu=\nu_3$. Thus, strictly speaking, we do not have a resonance[35] at $\nu=\nu_3$.

For $0<\Gamma<\Gamma_{\text{crit}}$ there is no bound state, and δ_0^0 starts from zero at $\nu=0$ stays positive, and does not pass through $\pi/2$. In the repulsive case $\pi/F'(\nu_1)<\Gamma<0$ the phase shift δ_0^0 starts from zero at $\nu=0$ and stays negative. The case $\Gamma<\pi/F'(\nu_1)$ is not of physical significance, since $D(\nu)$ then has a zero to the left of ν_1. In *all* cases δ_0^0 goes to zero like $(\text{const})/\nu$ as $\nu\to\infty$.

(viii) Subtractions

Since $\text{Im}f_+^0(t')$ is diverging like $|t'|$ near $t'=-25\mu^2$, and $D(\nu')\to 1-(\Gamma/\pi)F'(\nu_1)$ as $\nu'\to-\infty$, we have to make two subtractions in (43). These are made at $t=0$. One subtraction gives

$$f_+^0(t)=\frac{1}{D(\nu)}\Big[D(\nu=-1)\,\text{Re}f_+^0(t=0)+\frac{t}{\pi}P\int_{-\infty}^{a}dt'\,\frac{D(\nu')\,\text{Im}f_+^0(t')}{t'(t'-t)}\Big]. \tag{51}$$

The second subtraction gives

$$f_+^0(t)=\frac{1}{D(\nu)}\Big[D(\nu=-1)\,\text{Re}f_+^0(t=0)+t\frac{\partial}{\partial t''}(D(\nu'')\,\text{Re}f_+^0(t''))_{t''=0}+\frac{1}{\pi}t^2\frac{\partial}{\partial t''}P\int_{-\infty}^{a}dt'\,\frac{D(\nu')\,\text{Im}f_+^0(t')}{(t'-t'')(t'-t)}\Big|_{t''=0}\Big]. \tag{52}$$

In the second term on the right, $t''=4(1+\nu'')$.

We require the subtraction constants $\text{Re}f_+^0(0)$ and $(\partial/\partial t)\,\text{Re}f_+^0(t)|_{t=0}$. These have been evaluated by Menotti[36] from the forward $\pi-N$ scattering data using an extension of the method of Ball and Wong.[27] He gets

$$\text{Re}f_+^0(0)=-1.9\pm2, \tag{53}$$
$$\text{Re}f_+^{0\prime}(0)=2.8\pm0.9. \tag{54}$$

(The units $\hbar=c=\mu=1$ are used in numerical results throughout.) In this evaluation the α_{33} and the s-wave $\pi-N$ phase shifts are important. Also the small p-wave scattering lengths have to be used, and uncertainties in these are included in the estimated errors. The error in $\text{Re}f_+^0(0)$ is large because terms of the order of 100 cancel in this calculation. In the calculation of $\text{Re}f_+^{0\prime}(0)$ there is no cancellation of large terms. In evaluating the dispersion relation (52) the integral dominates for low values of t ($t>4$); in this term the Born contribution to $\text{Im}f_+^0(t')$ is predominant, so the value of the integral is readily determined to high accuracy. For large t the term in (52) which is linear in t will dominate. Comparatively large errors in this term have a small effect on the discrepancies because of the small values of the kernels $K^{(+)}(s,t)$ for large t (cf. Figs. 11 and 12).

(ix) Results of the N/D Pole Method

In Figs. 14 and 15 we show fits to the discrepancies $\Delta_0^{(+)}(s)$, $\Delta_{1/2}^{(+)}(s)$, and $\Delta_{3/2}^{(+)}(s)$ using the two parameter form $N(\nu)=\Gamma/(\nu-\nu_1)$. In fitting the discrep-

[35] A pole in the scattering amplitude on an unphysical sheet in the lower half plane ($\text{Im}\sqrt{\nu}<0$) will always give a phase shift which *increases* through $\pi/2$.

[36] P. Menotti, Nuovo cimento **23**, 931 (1962).

[37] J. S. Ball and D. Y. Wong, Phys. Rev. Letters **6**, 29 (1961).

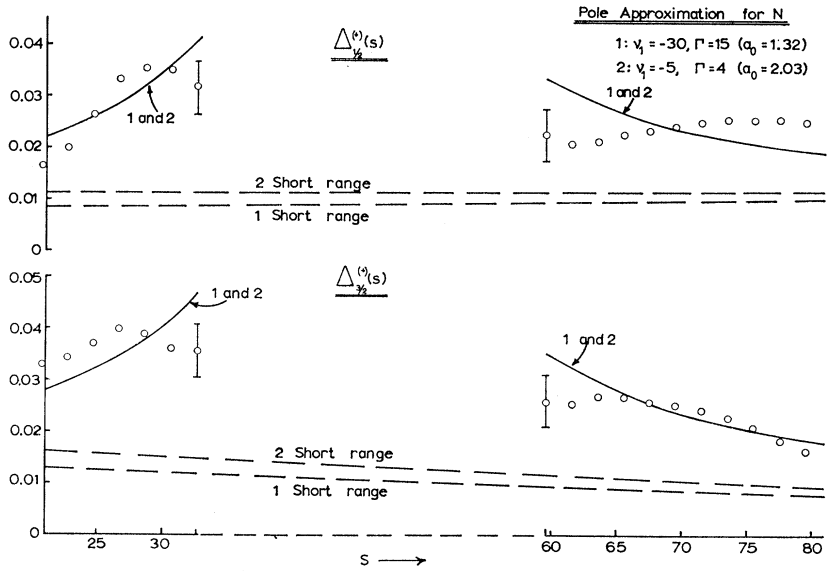

FIG. 15. The N/D pole approximation fits to the p-wave discrepancies $\Delta_{1/2}{}^{(+)}(s)$ and $\Delta_{3/2}{}^{(+)}(s)$ are given by the solid lines. The broken lines are the corresponding short-range parts. The circles indicate the experimental values calculated in Sec. 2.

ancies we first calculate the $\pi-\pi$ contribution coming from the front of the circle ($|\arg s| \leqslant 66°$) for a particular choice of Γ and ν_1. The remaining parts of the discrepancies are then fitted by *linear* short-range terms in the following way:

(i) $\Delta_0{}^{(+)}(s)$. Here we expect the threshold terms to be fairly accurate, and we fit the linear short-range term $a+bs$ at the two thresholds $s=(M\pm\mu)^2$.

(ii) $\Delta_{1/2}{}^{(+)}(s)$ and $\Delta_{3/2}{}^{(+)}(s)$. We assume that the errors at the two thresholds are due mainly to errors in the p-wave scattering lengths [see Sec. 3(xii) below]. Thus the errors in $\Delta_{1/2}{}^{(+)}(s)$ and $\Delta_{3/2}{}^{(+)}(s)$ at $s=(M-\mu)^2$ are related to those at $s=(M+\mu)^2$ (see Table I for details). Consequently, in each case only one parameter is needed to determine the linear short-range term, and this is obtained by fitting the discrepancies at $s=69$ (i.e., about 100 MeV) where we have accurate experimental confirmation of Woolcock's values of $\mathrm{Re}p_{1/2}{}^{(+)}$ and $\mathrm{Re}p_{3/2}{}^{(+)}$. It should be noted that the short-range terms are small and vary very slowly with s.

Reasonable fits to the discrepancies cannot be obtained for $\nu_1>-5$. However as ν_1 decreases below -5 there is a slight improvement in the goodness of the fit over that for $\nu_1=-5$. Figures 14 and 15 show the curves corresponding to scattering lengths $a_0=2$ ($\nu_1=-5$) and $a_0=1.3$ ($\nu_1=-30$) (a_0 is in units of $\hbar/\mu c$). The agreement with the experimental values is good; even for the p-wave discrepancies the difference between the experimental and theoretical values is never more than twice the standard errors in the p-wave $\pi-N$ data. Slightly better fits can be obtained with smaller values of a_0 and even more negative values of ν_1.

This tendency to get large negative values of ν_1 from our analysis suggests that we are meeting the same difficulty as occurs in the solution of the dynamical equations for $\pi-\pi$ scattering.[38] There it appears that the nearby part of the left-hand cut does not play a significant role in determining low-energy $\pi-\pi$ scattering. It may be that the position of the pole in our s-wave $\pi-\pi$ solution is far to the left for the same reason as has been suggested by Frazer[39] in another connection. If $N(\nu)$ for $\nu<-1$ has an attractive and a repulsive part, both occurring for moderate values of $-\nu$, approximating by a single pole as in (45) could lead to large values of $-\nu_1$.

The $\pi-\pi$ phase shifts $\delta_0{}^0(t)$ corresponding to our solutions are shown in Fig. 16. In each case $\Gamma>0$, but there is no bound state. General features common to the phase shifts $\delta_0{}^0(t)$ are that they rise to a maximum value of about 30° and then fall off to about 15° by $t=50$ ($q_3=3.39$). As ν_1 becomes more negative the energy at which $\delta_0{}^0(t)$ is maximum increases, reaching $t=8$ ($q_3=1$) for $\nu_1=-30$. Improved fits to the discrepancies can be obtained if $\delta_0{}^0(t)$ rises more slowly (corresponding to $a_0<1.3$) reaching a maximum of about 30° for $t>10$ ($q_3>1.24$). This corresponds to large negative values of ν_1.

(x) The Conformal Transformation Method

We saw in Sec. 3(v) that the discrepancies $\Delta^{(+)}(s)$ only determine certain "moments" of the helicity

TABLE I. Contributions from the p-wave scattering lengths $a_{2T,2J}$ to $\mathrm{Re}p_{2T,2J}$ at the thresholds $s=(M\pm\mu)^2$. Terms of relative order $(\mu/M)^2$ have been ignored at $s=(M-\mu)^2$.

	$s=(M+\mu)^2$	$s=(M-\mu)^2$
$\mathrm{Re}p_{3/2}{}^{(+)}$	$(1/3)(a_{13}+2a_{33})$	$(1/9)(a_{13}+2a_{33})+(2/9)(a_{11}+2a_{31})$
$\mathrm{Re}p_{1/2}{}^{(+)}$	$(1/3)(a_{11}+2a_{31})$	$(4/9)(a_{13}+2a_{33})-(1/9)(a_{11}+2a_{31})$
$\mathrm{Re}p_{3/2}{}^{(-)}$	$(1/3)(a_{13}-a_{33})$	$-(1/9)(a_{13}-a_{33})-(2/9)(a_{11}-a_{31})$
$\mathrm{Re}p_{1/2}{}^{(-)}$	$(1/3)(a_{11}-a_{31})$	$-(4/9)(a_{13}-a_{33})+(1/9)(a_{11}-a_{31})$

[38] J. S. Ball and D. Y. Wong, Phys. Rev. Letters 7, 390 (1961).

[39] See W. R. Frazer, in *Dispersion Relations*, edited by G. R. Screaton (Oliver & Boyd, Edinburgh, 1960), p. 256.

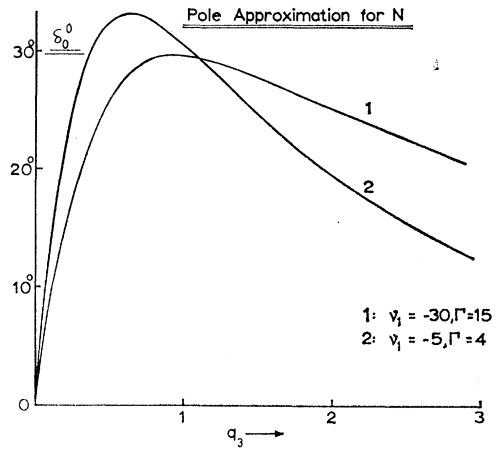

FIG. 16. The $T=0$ s-wave $\pi-\pi$ phase shifts for our N/D pole approximations. q_3 is the pion momentum in the c.m. system in units $\hbar=\mu=c=1$.

amplitude $\mathrm{Im}f_+^0(t)$ for $t\geqslant 4$. It is therefore of interest to show some other forms of $\delta_0^0(t)$ which give agreement with the low-energy $\pi-N$ data. For this purpose we use the conformal mapping method of Ciulli and Fischer[40] and Frazer[41] to generate functions $D(\nu)$ which give simple forms of $\delta_0^0(t)$. Equation (52) then gives $\mathrm{Im}f_+^0(t)$ for $t\geqslant 4$. We rely on the fact, which was shown by the original form of the Omnès method,[30] that $\mathrm{Im}f_+^0(t)$ for $t\geqslant 4$ is determined uniquely by knowing $\delta_0^0(t)$ for $t\geqslant 4$ and $\mathrm{Im}f_+^0(t)$ for $t\leqslant a=3.98$.

In the low-order approximations which we use, the numerator functions $N(\nu)$ do not appear to be physically significant. It would be necessary to go to higher order approximations to obtain values of $\mathrm{Im}A(\nu)$ for $\nu\leqslant -1$ which are like what we would expect from a dynamical theory of low-energy $\pi-\pi$ interactions. In the present section we use the conformal mapping method merely to exhibit simple forms of $\delta_0^0(t)$ which [together with our values of $\mathrm{Im}f_+^0(t)$ for $t\leqslant a$] give the observed discrepancies. It will be seen that there are considerable similarities between the phases $\delta_0^0(t)$ derived in this way and the values derived above by the N/D pole method.

The transformation

$$\eta=[1-(\nu+1)^{1/2}]/[1+(\nu+1)^{1/2}] \tag{55}$$

maps the top sheet of the ν plane cut along $-\infty\leqslant\nu\leqslant -1$ into the interior of the circle $|\eta|\leqslant 1$. Writing

$$\nu=-1+re^{i\vartheta}, \tag{56}$$

where $r\geqslant 0$ and $-\pi\leqslant\vartheta\leqslant\pi$, it is seen that the upper side of the cut $-\infty\leqslant\nu\leqslant -1$ goes into

$$\eta=\frac{1-ir^{1/2}}{1+ir^{1/2}}=\exp(i\psi),$$

where $\tan(\psi/2)=-r^{1/2}$ and the lower side of the cut goes into $\eta=\exp(-i\psi)$. The segments of the real axis $-1\leqslant\nu\leqslant 0$ and $0\leqslant\nu\leqslant\infty$ go into the segments of the diameter $0\leqslant\eta\leqslant 1$ and $-1\leqslant\eta\leqslant 0$, respectively. Figure 17 shows the transformed plane. We notice that near $\nu=0$, $\eta=-\frac{1}{4}\nu+O(\nu^2)$.

The phase shift $\delta_0^0(t)$ is generated by using

$$N(\nu)=\alpha_0+\alpha_1\eta+\alpha_2\eta^2+\cdots, \tag{57}$$

where α_0, α_1, $\alpha_2\cdots$ are real parameters. This gives $\mathrm{Im}N(\nu)=0$ on $-1\leqslant\nu\leqslant\infty$. The discontinuity in $N(\nu)$ across the cut $-\infty\leqslant\nu\leqslant -1$ is $2i\,\mathrm{Im}N(\nu)$ where

$$\mathrm{Im}N(\nu)=\alpha_1\sin\psi+\alpha_2\sin(2\psi)+\cdots. \tag{58}$$

For example using only the first two terms in (57), viz., $N(\nu)=\alpha_0+\alpha_1\eta$, we get

$$\mathrm{Im}N(\nu)=-2\alpha_1 r^{1/2}/(1+r). \quad (-\infty\leqslant\nu\leqslant -1) \tag{59}$$

In this case $|\mathrm{Im}N(\nu)|$ is greatest at $r=1$, i.e., $\nu=-2$. We shall use the form $N(\nu)=\alpha_0+\alpha_1\eta$ to fit our results.

The denominator function is given by (41), and it is convenient to subtract at $\nu_0=0$, so that

$$D(\nu)=1-\frac{\nu}{\pi}\int_0^\infty d\nu'\,\frac{1}{[\nu'(\nu'+1)]^{1/2}}\,\frac{N(\nu')}{\nu'-\nu}. \tag{60}$$

Thus $D(0)=1$. Using a finite number of terms in (57), $N(\nu)$ is bounded, and the integral in (60) converges well.

A Special Case

An interesting special case occurs if we use only the first term in (57), i.e., $N(\nu)=\alpha_0$. Then

$$D(\nu)=1-\frac{\alpha_0}{\pi}\nu\int_0^\infty\frac{d\nu'}{(\nu'(\nu'+1))^{1/2}}\,\frac{1}{\nu'-\nu}. \tag{61}$$

A simple calculation shows that in the notation of

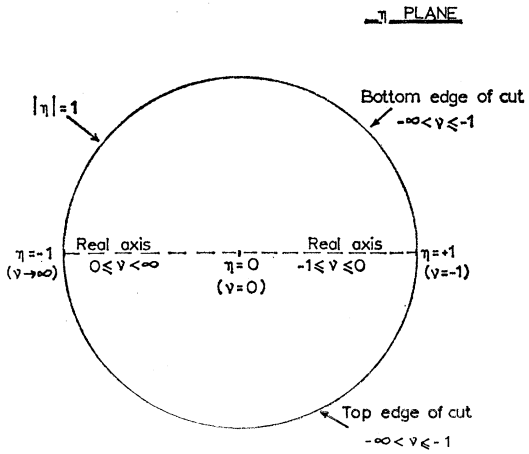

FIG. 17. The transformation of the top sheet of the cut ν plane into the circle $|\eta|=1$ given by Eq. (55).

[40] S. Ciulli and J. Fischer, Nuclear Phys. **24**, 465 (1961).
[41] W. R. Frazer, Phys. Rev. **123**, 2180 (1961).

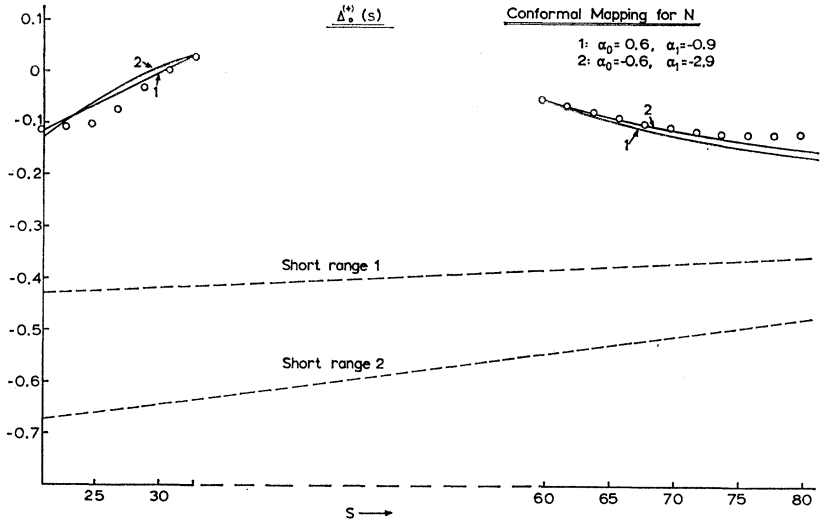

FIG. 18. The conformal mapping solution fits to the s-wave discrepancy $\Delta_0^{(+)}(s)$ are given by the solid curves. The broken lines are the corresponding short-range parts. The circles indicate the experimental values. The parameters $\alpha_0=a_0$ and α_1, refer to Eq. (57).

Appendix I,

$$\mathrm{Re}D(\nu)=1+\frac{\alpha_0}{\pi}F(\nu). \tag{62}$$

For $\nu\to\pm\infty$, we have

$$\mathrm{Re}D(\nu)\to\frac{\alpha_0}{\pi}\ln(4\nu)\quad\text{as}\quad\nu\to+\infty$$

and (63)

$$D(\nu)\to\frac{\alpha_0}{\pi}\ln(-4\nu)\quad\text{as}\quad\nu\to-\infty.$$

The divergence of $|D(\nu)|$ as $\ln|\nu|$ when $|\nu|\to\infty$ does not invalidate the derivation of (61) since the contribution from the circle at infinity vanishes due to the subtraction in (60). The corresponding dispersion relation for $N(\nu)$ also requires one subtraction, and in this special case the integral vanishes and the result $N(\nu)=\alpha_0$ is given by the subtraction constant.

Also

$$[\nu/(\nu+1)]^{1/2}\cot\delta_0^0=1/\alpha_0+(1/\pi)F(\nu). \tag{64}$$

Since $F(\nu)\geqslant 0$ (the equality occurring at $\nu=0$) for $\alpha_0>0$, δ_0^0 is positive and does not reach $\pi/2$; also $D(\nu)$ does not vanish on the negative real axis $\nu\leqslant 0$. For $\alpha_0<0$, $\cot\delta_0^0$ is negative for small ν and it has one zero. Also in this case, by (62), $D(\nu)$ has one zero on $-\infty\leqslant\nu\leqslant 0$. So for $\alpha_0<0$ there is a bound state and δ_0^0 drops from π at $\nu=0$ and falls through $\pi/2$ as ν increases. In both cases δ_0^0 behaves like $\pi/\ln(4\nu)$ for sufficiently large ν.

(xi) Results of the Conformal Mapping Method

In Figs. 18 and 19, we show fits to the discrepancies $\Delta_0^{(+)}(s)$, $\Delta_{1/2}^{(+)}(s)$, and $\Delta_{3/2}^{(+)}(s)$ using the two parameter form $N(\nu)=\alpha_0+\alpha_1\eta$. The method of fitting is similar to that used for the N/D pole method. Reason-

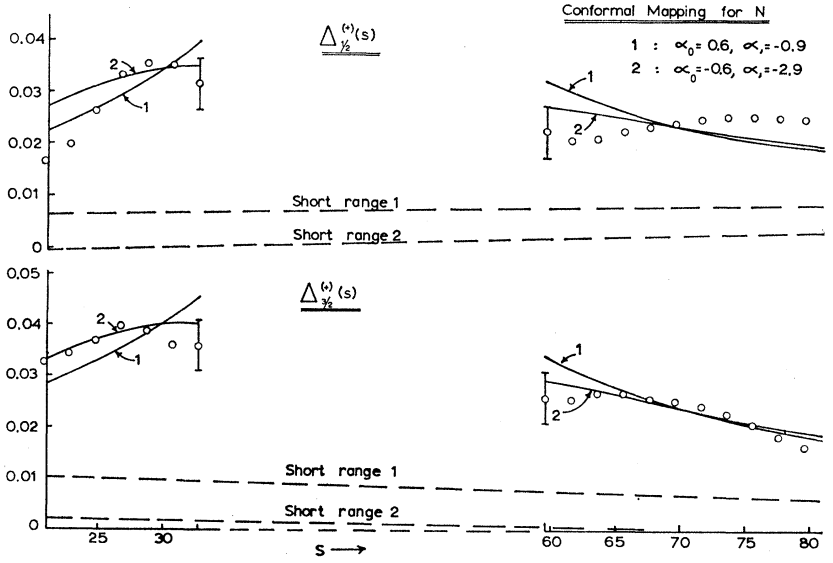

FIG. 19. The conformal mapping solution fits to the p-wave discrepancies $\Delta_{1/2}^{(+)}(s)$ and $\Delta_{3/2}^{(+)}(s)$ are given by the solid curves. The broken lines are the corresponding short range parts. The circles indicate the experimental values.

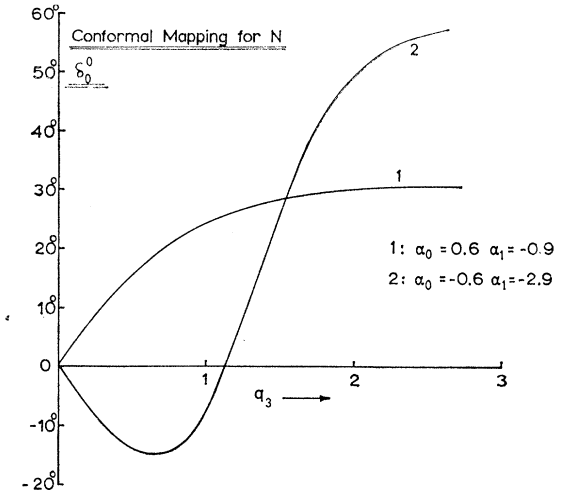

FIG. 20. The $T=0$ s-wave $\pi-\pi$ phase shifts for our conformal mapping solutions. q_3 is the pion momentum in the c.m. system.

able fits to $\Delta_0^{(+)}(s)$ are obtained for α_0 in the range $-1<\alpha_0<1$ Solution (1) ($\alpha_0=0.6$, $\alpha_1=-0.9$) gives the best fit to $\Delta_0^{(+)}(s)$ near $s=32.7$, while solution (2) ($\alpha_0=-0.6$, $\alpha_1=-2.9$) gives the best fit to $\Delta_0^{(+)}(s)$ near $s=59.6$ and also gives better fits to $\Delta_{1/2}^{(+)}(s)$ and $\Delta_{3/2}^{(+)}(s)$.

The corresponding $\pi-\pi$ phase shifts $\delta_0^0(t)$ are shown in Fig. 20. Solution (1) has the scattering length $a_0=0.6(\hbar/\mu c)$, and δ_0^0 is everywhere positive, rising to between 25° and 30° for $t>9$. Solution (2) has the scattering length $a_0=-0.6(\hbar/\mu c)$ and δ_0^0 is negative for $4<t<9.5 (0<q_3<1.17)$. For larger values of t, δ_0^0 is positive and it rises to between 50° and 60° for $t>9.5$ ($q_3>1.17$). It will be seen that, in general, the phase shift given by the two parameter conformal mapping method does not fall off as rapidly for the larger values of $t(30<t<50$ or $2.55<q_3<3.39)$, as that given by the N/D pole method. For both the solutions (1) and (2) $D(\nu)$ has no zero on the negative real axis, so there is no bound state. In both solutions $|\delta_0^0|$ never reaches $\pi/2$.

Thus we can choose a two-parameter fit of type (1) which gives good agreement with the s-wave discrepancy $\Delta_0^{(+)}(s)$. [The disagreement between the theoretical and experimental values of $\Delta_0^{(+)}(s)$ for $s>70$ may be due either to inaccurate values of the s-wave phase shifts α_1, α_3 above 200 MeV, or to the severe restriction imposed by using a linear short-range term.] As was explained in Sec. 3(ix) above, only one arbitrary parameter is involved in each of the short-range terms in the case of the p-wave discrepancies. The same values of $\delta_0^0(t)$ now give good agreement with $\Delta_{3/2}^{(+)}(s)$, the difference between experimental and theoretical values being nowhere greater than twice the estimated standard errors in the p-wave $\pi-N$ data. For $\Delta_{1/2}^{(+)}(s)$ the agreement is not so good, but this is not surprising since the experimental determination of the p-wave phase shifts α_{11} and α_{31} is particularly difficult.

Solution (2) partly allows for the fact that the p-wave experimental values of $\Delta_j^{(+)}(s)$ ($j=\frac{1}{2},\frac{3}{2}$) all fall below solution (1) near the two thresholds $s=(M\pm\mu)^2$. Solution (2) gives better agreement with $\Delta_0^{(+)}(s)$ in the region $59.6<s<70$ and it gives much better agreement with $\Delta_{3/2}^{(+)}(s)$. For $\Delta_{1/2}^{(+)}(s)$ the agreement is not so good, but the fit is within the estimated errors. In all the p-wave cases the short-range term is small and varies very slowly with s.

A common feature of our solutions for $\delta_0^0(t)$ obtained both by the N/D pole method and the conformal method is that the phase shift $\delta_0^0(t)$ is positive over the greater part of the range $4\leqslant t\leqslant 30$ ($0\leqslant q_3\leqslant 2.55$) and it rises to around 30° (or more) for moderate values of t ($10\lesssim t\leqslant 25$, i.e., $1.22\lesssim q_3\leqslant 2.29$). The only ambiguity in the general behavior of $\delta_0^0(t)$ is the possibility that it becomes negative for small t. It is clear that such a change in sign of $\delta_0^0(t)$ would not be easy to understand on the basis of a dynamical theory of the $\pi-\pi$ interaction.[42] We therefore examine what changes are required in the $\pi-N$ p-wave scattering lengths to remove all support for solutions in which $\delta_0^0(t)$ has a zero.

(xii) Behavior of $\Delta_{1/2}^{(\pm)}(s)$ and $\Delta_{3/2}^{(\pm)}(s)$ near the Thresholds

Apart from terms which vary comparatively slowly with s, the values of $\Delta_j^{(\pm)}(s)$ near the thresholds $s=(M+\mu)^2$ and $s=(M-\mu)^2$ are mainly determined by the Born terms, the (direct and crossed) α_{33} terms and $\mathrm{Re}p_{2T,2J}(s)$. The first two can be calculated accurately, so it is reasonable to blame any errors[43] on the values of $\mathrm{Re}p_{2T,2J}(s)$ near the thresholds. This suggests that near $s=(M\pm\mu)^2$ the main source of error is the values of $a_{2T,2J}$—the p-wave $\pi-N$ scattering lengths—which are given in (16). In Table I we show the contributions of the p-wave scattering lengths to $\mathrm{Re}p_{2T,2J}(s)$ near the thresholds; there are corrections of relative order (μ^2/M^2) at $s=(M-\mu)^2$ which we have not included.

By changing the values of $a_{13}+2a_{33}$, $a_{11}+2a_{31}$ we can bring the experimental values of $\Delta_{1/2}^{(+)}(s)$ and $\Delta_{3/2}^{(+)}(s)$ at $s=(M\pm\mu)^2$ into agreement with the values given by solution (1) (Fig. 19). For this purpose it is necessary to increase $a_{13}+2a_{33}$ and $a_{11}+2a_{31}$ by 0.025 and 0.030, respectively. These changes in the scattering lengths also imply small changes in Woolcock's p-wave $\pi-N$ phase shifts[9] in the region 0–100 MeV, and these would be such as to improve the agreement between the experimental values of $\Delta_{1/2}^{(+)}(s)$ and $\Delta_{3/2}^{(+)}(s)$ and the solution (1) values[44] shown in Fig. 19 in the regions

[42] We have not attempted to find such a solution by the direct N/D method since this would require two poles in $N(\nu)$, i.e., a 4-parameter fit.

[43] The contribution of the s-wave $\pi-N$ phases α_1 and α_3 via $\mathrm{Im}p_{2T,2J}(s)$ near $s=(M-\mu)^2$ is unlikely to lead to appreciable errors in $\Delta_j^{(\pm)}(s)$ near $s=(M-\mu)^2$. The d-wave $\pi-N$ contributions are unimportant near $s=(M-\mu)^2$.

[44] Small adjustments in the short-range terms might also be made.

$27 \leqslant s \leqslant 32.7$ and $59.6 \leqslant s \leqslant 67$. Agreement with the N/D pole solutions (Fig. 15) would similarly be improved.

$\Delta_{1/2}^{(-)}(s)$ *and* $\Delta_{3/2}^{(-)}(s)$ *near the Thresholds*

If the kinks in the experimental values of the discrepancies $\Delta_j^{(+)}(s)$ $(j=\frac{1}{2}, \frac{3}{2})$ near $s=(M\pm\mu)^2$ are due to small errors in the scattering lengths $a_{2T,2J}$ the same might be true for $\Delta_j^{(-)}(s)$ $(j=\frac{1}{2}, \frac{3}{2})$. As will be seen in Sec. 4(ii) and Fig. 22 below, there is better agreement between the theoretical and experimental values of $\Delta_j^{(-)}(s)$ $(j=\frac{1}{2}, \frac{3}{2})$ near $s=(M\pm\mu)^2$ than there is in the case of $\Delta_j^{(+)}(s)$. It will be seen by looking at Fig. 22 and Table I that in the case of $\Delta_j^{(-)}(s)$ $(j=\frac{1}{2}, \frac{3}{2})$ the agreement in the physical and crossed regions can be made even better by increasing $a_{13}-a_{33}$ and $a_{11}-a_{31}$ by 0.009 and 0.007, respectively.

Combining these changes in the (+) and (−) cases gives ($\hbar=\mu=c=1$)

$$\begin{aligned} a_{33} &= \ \ 0.219 \quad (0.214\pm0.004), \\ a_{11} &= -0.090 \ (-0.104\pm0.006), \\ a_{31} &= -0.032 \ (-0.040\pm0.004), \\ a_{13} &= -0.016 \ (-0.030\pm0.005). \end{aligned} \tag{65}$$

The values in parentheses are those due to Woolcock[29] [Eq. (16) above] which have been used in our calculations. It will be noted that only in the case of the smallest scattering length a_{13} is the change significantly more than two standard errors, while for a_{33}, which is the best known, it is just over one standard error.

(xiii) Strength of the Evidence for Solution (2)

We can now see the degree of accuracy which is required in the experimental and theoretical analysis of low-energy $\pi-N$ experiments if we are to assert firmly that $\delta_0^0(t)$ must change sign at low energies as in solution (2) [Sec. 3(xi) above and Fig. 20]. To assert this we would have to be certain that the values of $a_{2T,2J}$ on the left in (65) were incorrect and the values in brackets were correct. As we cannot be certain of this at present, the evidence for solutions of type (2) is weak.

The fact that smaller changes are suggested in the (−) combinations $a_{13}-a_{33}$, $a_{11}-a_{33}$ than in the (+) combinations $a_{13}+2a_{33}$, $a_{11}+2a_{33}$ may be related to the fact that the single variable dispersion relations used by Woolcock[9] in analyzing the low energy $\pi-N$ data, are more reliable in the (−) case than in the (+) case. In particular, the $A^{(+)}$ relation requires a subtraction and this is well known to give the possibility of errors in the resulting phase shifts.

The relation of our results for the $T=0$, $J=0$ $\pi-\pi$ phase shift to information obtained by other methods is discussed in Sec. 5(i) below.

4. THE $T=1$ π–π INTERACTION

(i) Narrow Resonance Approximation

First we show that the $\Delta^{(-)}(s)$ discrepancies can be reproduced very well by assuming there is a narrow resonance in the $T=1$, $J=1$ $\pi-\pi$ state. In order to link up with the nucleon form factors as well as $\pi-N$ scattering we require the pion electromagnetic form factor[45] $F_\pi(t)$. It is given by the dispersion relation

$$F_\pi(t)=1+\frac{t}{\pi}\int_{4\mu^2}^{\infty}\frac{\mathrm{Im}F_\pi(t')}{t'(t'-t)}dt'. \tag{66}$$

Also, by unitarity, we have for $4\mu^2 \leqslant t \leqslant 16\mu^2$,

$$\mathrm{Im}F_\pi(t)=(\text{real const})A_1^*(t)F_\pi(t), \tag{67}$$

where $A_1(t)$ is the invariant $\pi-\pi$ scattering amplitude for angular momentum $J=1$. In order to calculate the discrepancies we must know $F_\pi(t)$ accurately around $t=30\mu^2$, and approximately for values of t up to $50\mu^2$. Because the phase space for 4π processes is not large for $16\mu^2 \leqslant t \lesssim 30\mu^2$, we expect (67) to be approximately true in this range. However, this is not a large enough range of t for our purpose, and our neglect of inelastic processes (for larger t) may introduce errors into the results [a similar situation occurs in the calculation of $J_i(t)$ using Eq. (71) below]. These errors due to neglecting inelastic processes are probably more serious in the $T=1$ case, where we are interested in values of t around $30\mu^2$, than they were in the $T=0$ case [Sec. 3(v) above] where we only had to know the helicity amplitude $f_+^0(t)$ accurately for $t \leqslant 20\mu^2$.

For the present we assume Eq. (67) is valid for all values of t $(t \geqslant 4\mu^2)$ which we require. The $J=1$ $\pi-\pi$ phase shift $\delta_1(t)$ associated with a narrow resonance is given by

$$\exp(i\delta_1)\sin\delta_1=\frac{\gamma q_3{}^3}{t_R-t-i\gamma q_3{}^3}, \tag{68}$$

where q_3 is the pion momentum in the c.m. system. The resonance occurs at $t=t_R$ and has half-width (in units of t) $\gamma q_R{}^3$, where $t_R=4(\mu^2+q_R{}^2)$. In practice t_R and γ are of the order of magnitude of 30 and 0.3, respectively. By (66) and (67), we have

$$F_\pi(t)=(t_R-\gamma)/(t_R-t-i\gamma q_3{}^3). \tag{69}$$

From (66) or (69) it is seen that on the real axis $F_\pi(t)$ is real for $t<4\mu^2$.

Following Frazer and Fulco[28] we introduce the functions $\Gamma_i(t)$ $(i=1, 2)$. For $i=1$, 2 these functions are closely related, respectively, to the electric and magnetic nucleon isovector form factors $F_i{}^V(t)$. Also they are linear combinations of the helicity amplitudes $f_\pm{}^1(t)$ for $\pi+\pi \to N+\bar{N}$ in the $J=1$ state, so they give the $\Delta^{(-)}$ discrepancies.[46] We introduce the functions

[45] For details see W. R. Frazer, reference 39.
[46] See II and III for details.

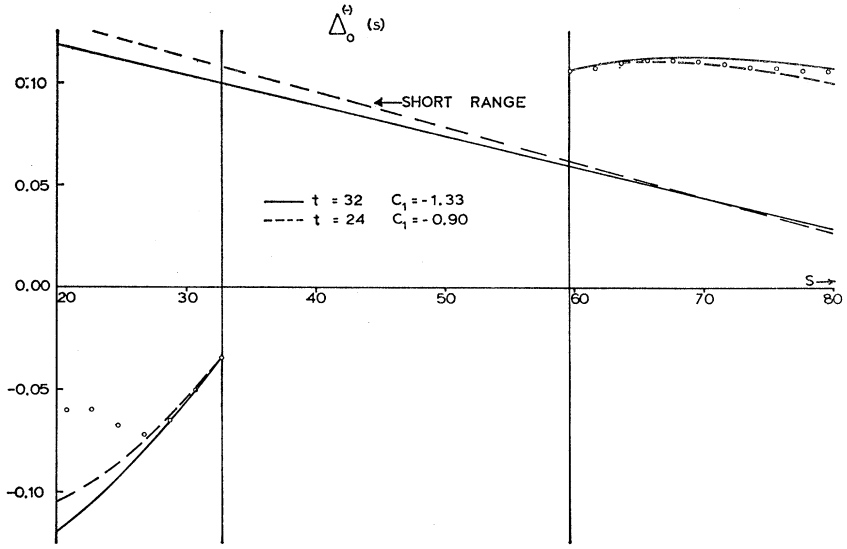

FIG. 21. The narrow $T=1$ $\pi-\pi$ resonance approximation fits to the s-wave discrepancy $\Delta_0^{(-)}(s)$ for $t_R=32$ and $t_R=24$. The corresponding short-range parts are also shown. The circles indicate the experimental values of $\Delta_0^{(-)}(s)$ calculated in Sec. 2.

$J_i(t)$

$$J_i(t)=\Gamma_i(t)/F_\pi(t). \quad (i=1,2) \tag{70}$$

From a unitary relation similar to (67) it follows that

$$J_i(t)=\frac{1}{\pi}\int_{-\infty}^{a}\frac{\mathrm{Im}J_i(t')}{t'-t}dt'. \tag{71}$$

Here we have again ignored difficulties, similar to those mentioned above, arising from the fact that the unitary relation is only strictly valid for $4\mu^2\leqslant t\leqslant 16\mu^2$.

Using methods similar to those discussed in Sec. 3(vi) above we can calculate $\mathrm{Im}\Gamma_i(t)$ for $-26\mu^2\leqslant t\leqslant a$ from our knowledge of the low-energy $\pi-N$ phase shifts and the coupling constant f^2. Thus from (71) (using subtractions if necessary) we can determine $J_i(t)$ for $t\gtrsim 4\mu^2$. For $t\gtrsim 4\mu^2$, $J_i(t)$ is real, and

$$\mathrm{Im}\Gamma_i(t)=\frac{J_i(t)\gamma q_3{}^3(t_R-\gamma)}{(t_R-t)^2+\gamma^2 q_3{}^6}. \quad (i=1,2) \tag{72}$$

So for a narrow resonance

$$\mathrm{Im}\Gamma_i(t)\simeq\pi t_R J_i(t_R)\delta(t-t_R). \tag{73}$$

This gives agreement with the usual δ-function approximation[47]

$$\mathrm{Im}\Gamma_i(t)=\pi C_i\delta(t-t_R), \quad (i=1,2) \tag{74}$$

on putting[48]

$$C_i=t_R J_i(t_R). \tag{75}$$

Equation (75) is the first consequence of the narrow-resonance hypothesis which can be checked. C_i is determined (experimentally) from our discrepancies $\Delta^{(-)}(s)$, and $J_i(t_R)$ is calculated directly from (71).

Nucleon Form Factors

Further consequences follow if we use the isovector nucleon form factors $F_i{}^V(t)$ $(i=1,2)$. These obey the dispersion relations[49]

$$\begin{aligned}\frac{2}{e}F_1{}^V(t)&=1+\frac{t}{\pi}\int_{4\mu^2}^{\infty}\frac{g_1(t')dt'}{t'(t'-t)},\\ \frac{2}{e}F_2{}^V(t)&=\frac{g}{M}+\frac{t}{\pi}\int_{4\mu^2}^{\infty}\frac{g_2(t')dt'}{t'(t'-t)}.\end{aligned} \tag{76}$$

Here $g=1.853$ is the (anomalous) gyromagnetic ratio, and

$$\begin{aligned}g_i(t)&=-2t^{-1/2}q_3{}^3F_\pi{}^*(t)F_i(t)\\ &=-2t^{-1/2}q_3{}^3|F_\pi(t)|^2J_i(t). \quad (i=1,2)\end{aligned} \tag{77}$$

For a narrow resonance,

$$g_i(t)=-(2\pi C_i t_R{}^{1/2}/\gamma)\delta(t-t_R). \tag{78}$$

Substituting in (76) gives

$$\begin{aligned}F_1{}^V(t)&=\frac{e}{2}\left(1+\frac{at}{t_R-t}\right),\\ F_2{}^V(t)&=\frac{eg}{2M}\left(1+\frac{bt}{t_R-t}\right),\end{aligned} \tag{79}$$

where

$$a=-2C_i/\gamma t_R{}^{1/2}, \quad b=-(M/g)2C_2/\gamma t_R{}^{1/2}. \tag{80}$$

Since, by observation,[50] $F_1{}^V(t)\simeq(M/g)F_2{}^V(t)$, we have

[47] J. Bowcock, N. Cottingham, and D. Lurié, Nuovo cimento **19**, 142 (1961).

[48] In II we used $\gamma_1=\pi C_1$, $\gamma_2=\pi MC_2$. The same notation is used by S. C. Frautschi and J. D. Walecka, Phys. Rev. **120**, 1486 1960).

[49] G. F. Chew, R. Karplus, S. Gasiorowicz, and F. Zachariasen, Phys. Rev. **110**, 265 (1958); P. Federbush, M. L. Goldberger, and S. Treiman, *ibid.* **112**, 642 (1958).

[50] R. Hofstadter and R. Herman, Phys. Rev. Letters **6**, 293 (1961).

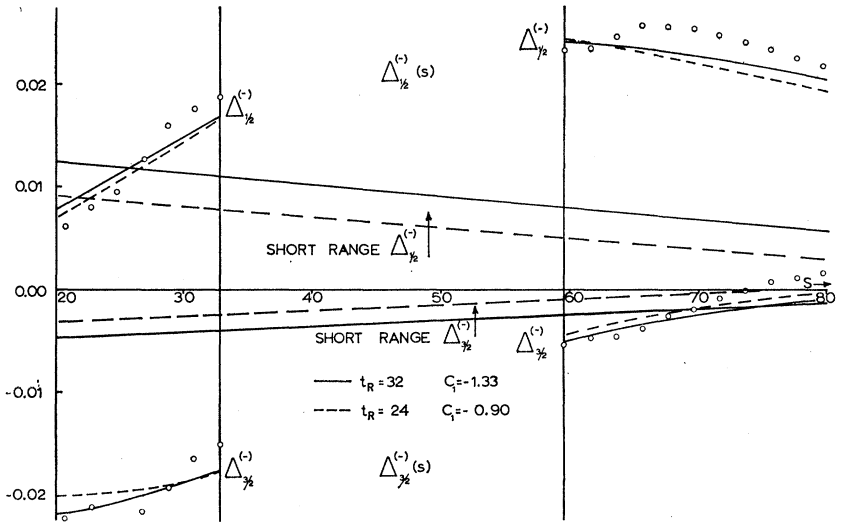

FIG. 22. The narrow $T=1$ $\pi-\pi$ resonance fits to the p-wave discrepancies $\Delta_{1/2}^{(-)}(s)$ and $\Delta_{3/2}^{(-)}(s)$ for $t_R=32$ and $t_R=24$. The corresponding short-range parts are also shown. The circles indicate the experimental values of $\Delta_i^{(-)}(s)$ calculated in Sec. 2.

$C_2 \simeq (g/M)C_1 = 0.27C_1$. Determining a from the nucleon form factors and C_1 from the discrepancies, Eq. (80) gives γ. This can be compared with the value of γ derived from the experimentally determined width of the $\pi-\pi$ resonance. This relationship is independent of the calculated values of $J_i(t)$.

Finally, the calculated values of $J_i(t)$ [obtained from Eq. (71)] should obey

$$J_2(t_R)/J_1(t_R) \simeq g/M. \tag{81}$$

(ii) Fitting the Discrepancies

The $\pi-\pi$ contributions to the $\Delta^{(-)}$ discrepancies were calculated using (74) with $C_2/C_1=0.27$. The integration extended over the arc $|\text{arg}s| \leqslant 66°$ of the circle $|s|=M^2-\mu^2$. The method of calculation has already been given in III. Again the short-range terms were restricted to the linear form $\alpha+\beta s$. Figures 21 and 22 show the experimental values of $\Delta_0^{(-)}(s)$, $\Delta_{1/2}^{(-)}(s)$, and $\Delta_{3/2}^{(-)}(s)$ and the calculated values for a narrow resonance at $t_R=32$ or $t_R=24$. We get $C_1=-1.33$ for $t_R=32$ and $C_1=-0.90$ for $t_R=24$. Tolerable, but not as good agreement is also obtained using $C_1=-0.53$ for $t_R=16$. Thus as has been noted above, the value of t_R is not readily determined from low-energy $\pi-N$ scattering.

In the case of the p-wave discrepancies, $\Delta_{1/2}^{(-)}(s)$ and $\Delta_{3/2}^{(-)}(s)$, the short range terms are fairly small and vary very slowly with s. This is particularly noticeable for $\Delta_{3/2}^{(-)}(s)$; in this case the $\pi-\pi$ interaction is the predominant effect. For $\Delta_{1/2}^{(-)}(s)$ it should be noted that the form of the discrepancy in the unphysical region ($s<32.7$) gives very strong confirmation that we are here detecting the $J=1$ $\pi-\pi$ effect. For $\Delta_0^{(-)}(s)$ there is a noticeable disagreement between the experimental and calculated values for $s<25$. As was pointed out in III this is not surprising since the errors in the experimental values of $\Delta_0^{(-)}(s)$ could well be large for $s<25$.

The value of C_1 is mainly limited by the fit to $\Delta_0^{(-)}(s)$ and removing the restriction that the short-range term in $\Delta_0^{(-)}(s)$ be linear in s could lead to somewhat smaller values of C_1. For this reason we reduce the above values of C_1 by 15%, and for $t_R=30$ we shall use $C_1=-1.05$. [In III we gave $C_1=-0.7\pm0.1$ for $t_R=25$. The value just given would correspond to $C_1=-0.80$ for $t_R=25$.] The errors in the values of C_1 thus adjusted are estimated to be $\pm 20\%$.

(iii) Experimental Data on the $T=1$ $\pi-\pi$ Interaction

Recent work[51–53] on the process $\pi+N \to \pi+\pi+N$ shows very clearly that there is a $\pi-\pi$ resonance (ρ) in the state $T=1$, $J=1$ having energy (765±10) MeV. The half-width (at half-height) is not accurately known yet, but a conservative estimate[54] suggests it is in the region 40–60 MeV. Similar conclusions follow from proton-antiproton annihilation experiments.[55] It has been suggested[55] that, in fact, there are two narrow resonances close together, but we shall not pursue that idea at present.

Further work on $\pi+N \to \pi+\pi+N$ has led to some evidence[56] in favor of a $T=1$ $\pi-\pi$ resonance (ζ) at (575±20) MeV. However, other experiments[51] do not show this low-energy resonance.

[51] Saclay, Orsay, Bari, Bologna Collaboration, Nuovo cimento **25**, 365 (1962).

[52] E. R. Erwin *et al.*, *Proceedings of the Aix-en-Provence International Conference on Elementary Particles* (Centre d'Etudes Nucleaires de Saclay, Seine et Oise, 1961), Vol. 1, 249; D. D. Carmody and R. T. Van de Walle, Phys. Rev. Letters **8**, 73 (1962).

[53] For earlier work see the references in III.

[54] See D. L. Stonehill and H. L. Kraybill (to be published).

[55] J. Button, G. R. Kalbfleisch, G. R. Lynch, B. C. Maglić, A. H. Rosenfeld, and M. L. Stevenson, Phys. Rev. **126**, 1858 (1962); and University of California Radiation Laboratory Report UCRL-9814 (unpublished).

[56] R. Barloutaud, J. Heughebaert, A. Leveque, and J. Meyer, Phys. Rev. Letters **8**, 32 (1962); V. P. Kenney *et al.*, Nuovo cimento **23**, 245 (1962); B. S. Zorn, Phys. Rev. Letters **8**, 282 (1962).

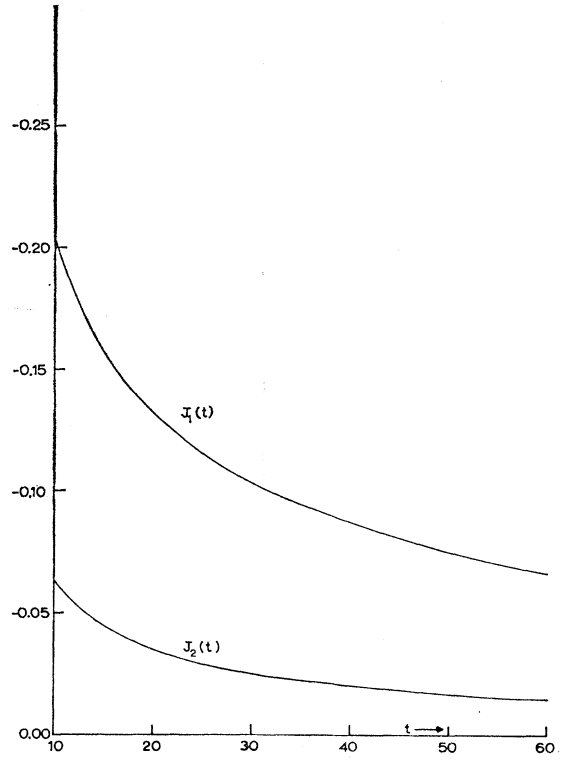

FIG. 23. Calculated values of the functions $J_1(t)$ and $J_2(t)$.

(iv) Calculation of $J_i(t)$

We have to find $J_i(t)$ for $t\geqslant 4$ using Eq. (71). The numerator in the integrand is $\mathrm{Im}\Gamma_i(t)/F_\pi(t)$, since $F_\pi(t)$ is real for $t<4$. $\mathrm{Im}\Gamma_i(t)$ has been calculated in the interval $-26\leqslant t\leqslant a$ by Frazer and Fulco.[57] In order that uncertainties in the values of $\mathrm{Im}\Gamma_i(t)$ for $t<-26$ should not make our calculation of $J_i(t)$ worthless, it is necessary either to make subtractions in (71) or to use some justifiable cutoff procedure. By the method of Ball and Wong[31] $\Gamma_i(0)$ and $\Gamma_i'(0)$ can be evaluated in terms of $\pi-N$ scattering data, and the subtractions in (71) are made at $t=0$. Vick[58] has recalculated these subtraction constants, getting

$$\begin{aligned}\Gamma_1(0)&=-0.1415,\\ \Gamma_2(0)&=+0.0088,\\ \Gamma_1'(0)&=+0.0409,\\ \Gamma_2'(0)&=-0.00586.\end{aligned}\tag{82}$$

Using these values and Eq. (69) with $t_R=30$, $\gamma=0.3$ [59] functions $J_i(t)$ are determined[58] for $t\geqslant 4$. Vick's result for $J_i(t)$ is shown in Fig. 23.

[57] See reference 28. $\mathrm{Im}\Gamma_i(t)$ has been recalculated using the latest $\pi-N$ low energy data.

[58] L. L. J. Vick (to be published).

[59] The values of $J_i(t)$ are insensitive to γ.

(v) Comparison of Experiment with Theory

We shall assume that the $T=1$, $J=1$ $\pi\pi$ resonance occurs at $t_R=30$ (767 MeV) and note that a half-width of 56 MeV would give $\gamma=0.30$. In Sec. 4(ii) above we saw that our discrepancies give $C_1=-1.05\pm0.2$ for $t_R=30$, and from Fig. 23 it is seen that the calculated value of $J_1(t=30)$ is -0.104. It follows from (75) that the calculated value of $J_1(t_R)$ is too large by a factor of 3. If we were to reduce t_R the disagreement would become greater as that reduces $|C_1|$ more rapidly than $t_R|J_1(t_R)|$. [Here the dependence of $J_1(t)$ on t_R has to be allowed for.]

Now we examine the relation (80) between the nucleon form factors and the discrepancies. This relation is independent of the calculated value of $J_i(t_R)$. To fit the form factors $F_i^V(t)$ with $t_R=30$ we use $a=1.6$ in Eq. (79). With $C_1=-1.05\pm0.2$ Eq. (80) gives $\gamma=0.24\pm0.05$, which is in reasonable agreement with the experimental value $0.22\leqslant\gamma\leqslant0.33$. Next we have Eq. (81). The ratio of the calculated values $J_2(t_R)/J_1(t_R)$ is 0.24, which is to be compared with the experimental value 0.27. The agreement here is not as good as one might hope.

Thus the relations (75) and (81) which involve the calculated values of $J_i(t_R)$ have not been verified with any precision. In Sec. 4(i) above we pointed out that errors could arise because inelastic processes, which may be important, have been ignored in the dispersion relation (71) (or in its subtracted forms). There are further possible reasons for this failure to verify (75) and (81). The only appreciable $T=1$ $\pi-\pi$ interaction about which we have firm and useful information is the resonance at the high energy $t_R\simeq30$. Thus, the continuation of $F_\pi(t)$ to negative values of t using Eq. (69) may involve appreciable errors.[60] Since the important values of t ($t\simeq t_R$) are so large, the evaluation of the subtracted form of the dispersion relation (71) may introduce substantial errors in $J_i(t)$ due to uncertainties in the subtraction constants $\mathrm{Re}\Gamma_i'(0)$ (or possibly due to uncertainties in $\mathrm{Im}\Gamma_i(t)$ for $t<a$). For example a 10% error in $\mathrm{Re}\Gamma_i'(0)$ would lead to a 100% error in $J_1(t_R)$ on using the double subtracted relation.

In short, any verification of Eqs. (75) and (81) is up against the difficulties usually encountered when dispersion relations are used at moderately high energies. These difficulties only refer to the calculated values of $J_i(t_R)$ obtained from Eq. (71). They do not in any way invalidate our identification of the $T=1$, $J=1$ $\pi-\pi$ effect in low-energy $\pi-N$ scattering, or its relation to the nucleon form factors and the observed $J=1$ $\pi-\pi$ resonance around 760 MeV through Eq. (80).

5. DISCUSSION OF THE RESULTS

We have shown how the dispersion relations for the s- and p-wave $\pi-N$ scattering amplitudes can be used

[60] For example, this would be the case if the $\pi-\pi$ phase shift descended to zero again at, say, $t=60\mu^2$.

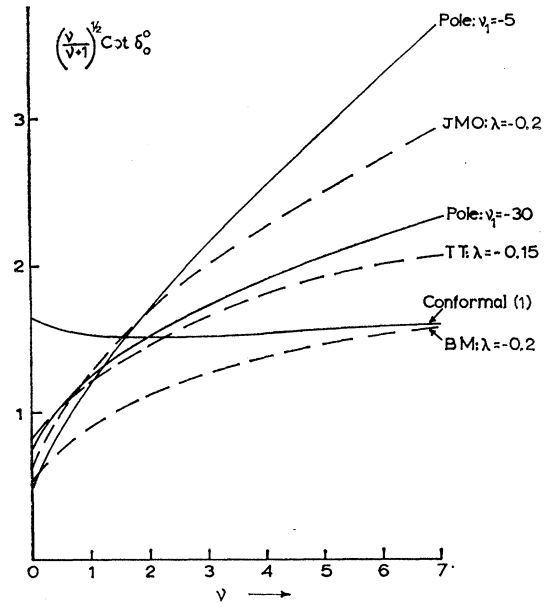

FIG. 24. The solid lines are the effective-range plot for our phase shifts δ_0^0 (cf. Figs. 16 and 20). The broken lines are the (JMO) $\lambda=-0.2$, (TT) $\lambda=-0.15$, and (BM) $\lambda=-0.2$ solutions of the Chew-Mandelstam equations.

to break down low-energy (lab energy $\leqslant 200$ MeV) $\pi-N$ scattering unambiguously into its main constituents: Born terms, $\pi-\pi$ interactions, short-range interactions. We have also seen that this yields valuable information about the low-energy $T=0$, $J=0$ $\pi-\pi$ interaction and some information about the $T=1$ $\pi-\pi$ interaction. We now examine the relation of our results to other information on $\pi-\pi$ and $\pi-N$ interactions.

(i) The $T=0$, $J=0$ π–π Interaction

We saw in Sec. 3 that several sets of $T=0$, $J=0$ $\pi-\pi$ phase shifts δ_0^0 give good agreement with the three *discrepancies* $\Delta^{(+)}(s)$ which we derived from the experimental data on s- and p-wave $\pi-N$ scattering. These sets of values of δ_0^0 are given by the N/D pole solutions [Sec. 3(ix)] having the pole at $\nu_1=-5$, -30, or $\nu_1\ll-30$ (cf. Fig. 16). Also, there is solution (1) (cf Fig. 20) of the conformal mapping method [Sec. 3(xi)]. The corresponding values of the $T=0$ s-wave $\pi-\pi$ scattering length a_0 are shown in Table II.

The values of a_0 are spread over a fairly wide range because low-energy $\pi-N$ scattering only depends on a weighted average of the $T=0$ $\pi-\pi$ interaction taken over an appreciable range of the $\pi-\pi$ energy. Thus a small value of a_0, as in conformal solution (1), is compensated by values of δ_0^0 which do not fall off noticeably at high $\pi-\pi$ energies (cf. Fig. 20).

Common features of the solutions mentioned above are that δ_0^0 is positive at all energies, and that δ_0^0 rises to around 25° or 30° at low pion energies. We conclude that there is a moderately strong attraction between two pions in the $T=0$, $J=0$ state at low energies.

Actually the N/D pole solutions with $\nu_1\lesssim-30$ and the conformal solution (1) give the best fits to our data.[61] Thus low-energy $\pi-N$ scattering really suggests a somewhat narrower range of values[62] of a_0 than that given in Table II, say,

$$0.6\lesssim a_0\lesssim 1.7. \tag{83}$$

Comparison with Solutions of the $\pi-\pi$ Equations

Recently solutions of the Chew-Mandelstam[63] equations for $\pi-\pi$ scattering have been derived by several authors.[64–68] These give a fairly strong $T=0$ s-wave $\pi-\pi$ attraction which is consistent[64] with the p-wave $\pi-\pi$ resonance.

In Fig. 24 we show the effective-range plot for δ_0^0 given by Bransden and Moffat (BM) with $\lambda=-0.2$, by Taylor and Truong (TT) with $\lambda=-0.15$, and by Jacob *et al.* (JMO) with $\lambda=-0.2$. λ is the $\pi-\pi$ coupling parameter. For comparison we also show our N/D pole solutions with $\nu_1=-5$ and $\nu_1=-30$, and the conformal solution (1).

Figure 24 can be used to pick out those solutions of the Chew-Mandelstam equations which are consistent with low-energy s- and p-wave $\pi-N$ scattering. For the range of values of λ which is of interest here, the (BM) and (TT) solutions are almost identical, and we do not distinguish between them. The (BM), or (TT), solution with $\lambda=-0.15$ is close to our N/D pole solution with $\nu_1=-30$.[69] Also, (TT) give[67] $a_0=1.2$ for

TABLE II. Values of the $T=0$ s-wave $\pi-\pi$ scattering length a_0 for our various solutions.

Solution	a_0 (in units $\hbar=c=\mu=1$)
N/D pole, $\nu_1=-5$	2.0
N/D pole, $\nu_1=-30$	1.3
N/D pole, $\nu_1<-30$	$1.0<a_0<1.3$
Conformal solution (1)	0.6

[61] We do not consider conformal mapping solution (2) which we exclude for the reasons stated in Sec. 3 (xiii).

[62] K. Ishida, A. Takahashi, and Y. Veda, Progr. Theoret. Phys. **23**, 731 (1960), and A. V. Efremov, V. A. Meshcheryakov, and D. V. Shirkov, Soviet Phys.—JETP **12**, 308, 766 (1961), obtained $a_0\cong 1$ from a dispersion relation method applied to the small p wave $\pi-N$ phase shifts.

[63] G. F. Chew and S. Mandelstam, Phys. Rev. **119**, 467 (1960); G. F. Chew, S. Mandelstam, and H. P. Noyes, *ibid.* **119**, 478 (1960).

[64] B. H. Bransden and J. W. Moffat, *Proceedings of the Aix-en-Provence International Conference on Elementary Particles* (Centre d'Etudes Nucleaires de Saclay, Seine et Oise, 1961), Vol. I, p. 343; Nuovo cimento **21**, 505 (1961); **23**, 598 (1962); Phys. Rev. Letters **8**, 145 (1962). We are indebted to Dr. Bransden for giving us further details of these calculations.

[65] M. Jacob, G. Mahoux, and R. Omnès, *Proceedings of the Aix-en-Provence International Conference on Elementary Particles* (Centre d'Etudes Nucleaires de Saclay, Seine et Oise, 1961), Vol. I, p. 331; Nuovo cimento **23**, 838 (1962).

[66] J. S. Ball and D. Y. Wong, Phys. Rev. Letters **7**, 390 (1961).

[67] J. G. Taylor and T. N. Truong, Nuovo cimento **25**, 946 (1962).

[68] See also V. V. Serebraykov and D. V. Shirkov, Zhur. Eksp. i Teoret. Fiz. **42**, 611 (1962).

[69] The agreement is even better for an N/D pole solution with $\nu_1<-30$.

$\lambda=-0.15$. The (JMO) solution with $\lambda=-0.2$ ($a_0=1.6$) is close to our N/D pole solution with $\nu_1=-5$. Our $\nu_1=-5$ solution is also in fair agreement with a (JMO) solution having slightly smaller $|\lambda|$. Our conformal mapping solution (1) is not in agreement with any of the (JMO), (BM), or (TT) solutions, as is to be expected from the way in which it is derived. Also, the published solutions of Ball and Wong[66] are not similar to any of our solutions.

We make the following deductions:

(a) If we fit to a (JMO) solution we have to use a slightly more negative value of λ than we require for fitting to (BM) and (TT). However, allowing for the divergence between these authors, our analysis of the $\pi-N$ data suggests that the $\pi-\pi$ coupling parameter is

$$\lambda=-0.18\pm0.05. \tag{84}$$

(b) If we add to our $\pi-N$ analysis the criterion that our solutions should be of the same general form as the solutions of the Chew-Mandelstam equations, then conformal solution (1) is to be excluded,[70] and the scattering length a_0 is determined much better than in Eq. (83). On this basis a rough estimate is

$$a_0=1.3\pm0.4. \tag{85}$$

The $p+d\rightarrow \mathrm{He}^3+(2\pi)$ Experiment

In this experiment[71] the momentum of the recoil He^3 is measured and a marked bump is found in the number of events occurring just beyond the two pion threshold. This could be caused by a strong $\pi-\pi$ attraction at low energies in the $T=0$, $J=0$ state, and early theoretical estimates suggested that a large $\pi-\pi$ scattering length $a_0\simeq2.5$ was required.[72]

Recently, using a new formulation for dealing with the final-state interaction, Jacob *et al.*[73] have obtained very good agreement with the results of the $p+d$ experiment by using the (JMO) phase shift, δ_0^0 with $\lambda=-0.2$ ($a_0=1.6$) shown in Fig. 24. The (JMO) phase shifts δ_0^0 for $\lambda=-0.22$ ($a_0=1.8$) and $\lambda=-0.18$ ($a_0=1.3$), respectively, give good and fairly good agreement with the $p+d$ experiment. The (JMO) phase shifts δ_0^0 are characterized by a comparatively large scattering length and a sharp drop in the values of δ_0^0 at high energies. The (BM) and (TT) sets of values of δ_0^0 do not have these properties to such an extent, and they are therefore not expected to give such good agreement with the results of the $p+d$ experiment. If δ_0^0 is more like the (JMO) solutions than the (BM), (TT) solutions, then the $p+d$ experiment is in good agreement with our analysis of $\pi-N$ scattering.

The Process $\pi+N\rightarrow\pi+\pi+N$

Analysis of the process $\pi+N\rightarrow\pi+\pi+N$ at low energies also gives information about the $\pi-\pi$ scattering lengths. Schnitzer[74] uses a model based on static theory[75] and applies it to data (differential and total cross sections) at (lab) energies between 360 and 500 MeV. He finds two possible sets of values (i) $a_0=0.50$, $a_1=0.07$, $a_2=0.16$; (ii) $a_0=0.65$, $a_1=0.07$, $a_2=-0.14$ where a_0 and a_2 are the $T=0$ and $T=2$ s-wave $\pi-\pi$ scattering lengths and a_1 is the $T=1$ p-wave $\pi-\pi$ scattering length. Ceolin and Stroffolini[76] examine the effect of peripheral interactions and analyze experimental data between 225 and 317 MeV. They find that a_0 must be less than one unit.

Thus, the analyses of the process $\pi+N\rightarrow\pi+\pi+N$ suggest that $a_0<1.0$. However there may be no contradiction between these results and the $p+d$ experiment, or a value of a_0 around 1.3. The analysis of Schnitzer is based on a $T=0$ $\pi-\pi$ interaction of the form $\lambda_s\phi^4$ the value of λ_s and hence of a_0, being determined from the $\pi+N\rightarrow\pi+\pi+N$ experimental results. The experiments used are well above the threshold for $\pi+N\rightarrow\pi+\pi+N$ (which is 171 MeV). From Fig. 16 it is seen that δ_0^0 rises steeply at very low energies and then falls off. Schnitzer's analysis relates to the region of energies where δ_0^0 is falling off, so he will underestimate a_0 [which is determined from $(\sin\delta_0^0)/q_3$, where q_3 is the pion momentum in $\pi-\pi$ scattering]. The analysis of Ceolin and Stroffolini does not appear to be self-consistent. Using their predictions for the total cross section[77] for $\pi^-+p\rightarrow\pi^-+\pi^++n$, we see that the data below 280 MeV do require $a_0<1.0$. However, two experimental points between 280 and 320 MeV require $a_0\simeq1.3$, while data[78] around 380 MeV suggest that $a_0\simeq2.6$.

Thus the main features of the $\pi+N\rightarrow\pi+\pi+N$ experiments[79] have not been shown to contradict our value $a_0=1.3\pm0.4$ given in Eq. (85).

[70] The (BM) solution with $\lambda=-0.1$ gives $a_0=0.67$ and puts the p-wave $\pi-\pi$ resonance at $t_R=25$. However this solution yields values of δ_0^0 which are too small to account for the size of the $T=0$ $\pi-\pi$ effect in $\pi-N$ scattering.

[71] A. Abashian, N. E. Booth, and K. M. Crowe, Phys. Rev. Letters **5**, 258 (1960).

[72] A. Abashian, N. E. Booth, and K. M. Crowe, Phys. Rev. Letters **7**, 35 (1961); B. R. Desai, *ibid.* **6**, 497 (1961). See also S. Fubini, *Proceedings of the Aix-en-Provence International Conference on Elementary Particles* (Centre d'Etudes Nucleaires de Saclay, Seine et Oise, 1961), Vol. II, p. 52.

[73] M. Jacob, G. Mahoux, and R. Omnes, Nuovo cimento **23**, 838 (1962).

[74] H. J. Schnitzer, Phys. Rev. **125**, 1059 (1962).

[75] C. J. Goebel and H. J. Schnitzer, Phys. Rev. **123**, 1021 (1961).

[76] C. Ceolin and R. Stroffolini, Nuovo cimento **22**, 437 (1961); S. Fubini, *Proceedings of the Aix-en-Provence International Conference on Elementary Particles* (Centre d'Etudes Nucleaires de Saclay, Seine et Oise, 1961), Vol. II, p. 52.

[77] See S. Fubini, reference 76, Fig. 12.

[78] For details of the experimental results see H. Schnitzer, reference 74.

[79] If the experimental data on the total cross sections for $\pi^-+p\rightarrow\pi^-+\pi^++n$ below 280 MeV, and its theoretical analyses (see references 74 and 76) are reliable then $a_0<1.0$ is favored.

τ-Decay

The original analysis of τ-decay events based on the work of Khuri and Treiman[80] gave $a_2-a_0\simeq 0.7$. The results of Schnitzer[74] above give $|a_2|\simeq 0.15$, and Kirz *et al.*[81] obtain $|a_2|\leqslant 0.15$ from a study of $\pi^++p\rightarrow\pi^++\pi^++n$. These results would contradict our value of a_0, [Eq. (85) above]. However, recent work by Bég and De Celles[82] shows that the situation is very different if the effects of the p-wave $\pi-\pi$ resonance (ρ) are included in the analysis of τ decay. They also give a rough estimate of the size of the effect. Using the values of a_0 and λ given by (85) and (84) and the parameters of the ρ resonance given in Sec. 4(iii), this estimate gives good agreement with the τ-decay data.

Conclusion

Our analysis of low-energy s- and p-wave $\pi-N$ scattering proves that there is a fairly strong $\pi-\pi$ attraction in the $T=0$ s state at low energies. Comparing our results (Fig. 24) with solutions of the Chew-Mandelstam equations for $\pi-\pi$ scattering, we get good agreement with the $T=0$ s-wave (BM)[64] and (TT)[67] solutions for $\lambda=-0.15$ ($a_0=1.2$) or with the (JMO)[65] solution for $\lambda=-0.20$ ($a_0=1.6$). The $p+d$ experiment favors this (JMO) solution,[73] while the $\pi+N\rightarrow\pi+\pi+N$ experiments possibly favor the (BM) and (TT) solutions. Our estimates of a_0 and λ are given in Eqs. (85) and (84).

(ii) The $T=1$ π–π Interaction

Our analysis of low-energy $\pi-N$ scattering can only give qualitative information about the values of t [$t=$(energy)^2] for which the $T=1$, $J=1$ $\pi-\pi$ interaction is strong [cf. Sec. 4(ii)]. However, the observed $T=1$, $J=1$ $\pi-\pi$ resonance (ρ) occurring at about 760 MeV would give rise to our low-energy $\pi-N$ results [in the (−) charge combination]. In particular Eq. (80), which relates (a) the magnitude of our discrepancies $\Delta^{(-)}(s)$ for s- and p-wave $\pi-N$ scattering, (b) the isovector nucleon form factors, (c) the observed position (t_R) and width (γ) of the resonance ρ, is satisfied by the data.

Relation (75) which gives the magnitude of the discrepancies $\Delta^{(-)}(s)$ in terms of the helicity amplitudes $f_{\pm}^1(t)$ for the process $\pi+\pi\rightarrow N+\bar{N}$ (via the functions $J_1(t)$ and $J_2(t)$), and Eq. (81) which relates the gyromagnetic ratio to $J_1(t_R)/J_2(t_R)$, are only satisfied qualitatively. This is attributed to errors in the calculation of $J_i(t)$ ($i=1, 2$) from the dispersion relation (71). Reasons were given in Sec. 4(v) for expecting that, with present techniques, the calculated values of $J_i(t_R)$ might be subject to appreciable errors. This does not invalidate the agreement with Eq. (80) mentioned in the previous paragraph, since that equation is independent of the calculated values of $J_i(t_R)$.

TABLE III. The first four rows give the various contributions to $\mathrm{Re}p_{2T,2J}=(\sin 2a_{2T,2J})/2q^3$ at the physical threshold. F is defined by (value at $s=59.6-$value at $s=80.6$)/(value at $s=59.6$ +value at $s=80.6$).

$2T, 2J$	Born (long range)	Crossed integral	Core	$T=0$ $\pi\pi$	$T=1$ $\pi\pi$	Rescattering
11	−0.202	0.026	0.026	0.024	0.032	0.003
31	−0.051	0.006	0.002	0.024	−0.016	0.001
13	−0.052	0.006	0.005	0.026	−0.005	0
33	+0.104	0.001	0.012	0.026	+0.003	0.079
$\|F\|$	0.4	0.2	∼0.1	∼0.4	0–1	···

Equation (75) does suggest that a $T=1$, $J=1$ $\pi-\pi$ resonance at 560 MeV (ζ), if it exists, does not have a large effect on low-energy $\pi-N$ scattering. As was shown in Sec. 4(ii), reducing the value of t_R will reduce the magnitude of the parameter C_1 more rapidly than $|t_RJ(t_R)|$ is decreased. If the ζ resonance contributes appreciably, then t_R has to be reduced to, say, 24 in order to give some mean energy for the $T=1$ $\pi-\pi$ interaction. As this noticeably increases the disagreement in (75), it is unlikely that ζ is important here.

Finally, we note that Schnitzer[74] obtained $a_1=0.07$ and Goebel and Schnitzer[75] got $a_1\simeq 0.04$ for the p-wave $\pi-\pi$ "scattering length." As was pointed out by Goebel and Schnitzer,[75] a_1 is so defined in their work that it will be appreciably greater than the actual scattering length, if the $T=1$ $\pi-\pi$ resonance occurs at a high energy. From Eq. (72) we see that the true scattering length is $a_1=\gamma/t_R\simeq 0.01$.

(iii) Breakdown of Low-Energy p-Wave π–N Scattering

In III (Sec. 7A and Fig. 10), low-energy s-wave $\pi-N$ scattering was resolved into constituent parts arising from the short-range $\pi-N$ interaction, the $T=0$ and $T=1$ $\pi-\pi$ interactions, and rescattering. That analysis is almost unaltered by our new calculations, and the results will not be repeated.

The results of Secs. 3 and 4 above make it possible to do a similar analysis for the p-wave $\pi-N$ phase shifts. This is done by picking out the contribution of the various terms in the dispersion relation (5) for the partial wave amplitude $\mathrm{Re}p_{2T,2J}=(\sin 2\alpha_{2T,2J})/2q^3$. Their values at the physical threshold are given in Table III. The separation of short-range terms (which we call *core* terms) and the $\pi-\pi$ terms was carried out with the aid of Figs. 15 and 22. The $T=0$ $\pi-\pi$ term is for the N/D pole solution with scattering length $a_0=1.3$ ($\nu_1=-30$) and the $T=1$ $\pi-\pi$ term is for $t_R\simeq 30$.

[80] N. N. Khuri and S. B. Treiman, Phys. Rev. **119**, 1115 (1960). See also F. Lomon, S. Morris, E. J. Irwin, and T. Truong, Ann. Phys. (New York) **13**, 359 (1961).
[81] J. Kirz, J. Schwartz, and R. D. Tripp, Phys. Rev. **126**, 763 (1962).
[82] M. A. B. Bég and P. C. De Celles, Phys. Rev. Letters **8**, 46 (1962).

The Born term here, and in what follows, is the long-range part arising from the pole $s=M^2$ and the short cut $(M-\mu^2/M)^2\leqslant s\leqslant M^2+2\mu^2$. The crossed integral is the contribution from the cut $0\leqslant s\leqslant(M-\mu)^2$. Except in the case of Rep_{33} it is mainly due to the crossed term coming from the $(\frac{3}{2},\frac{3}{2})$ resonance.[83] The core term comes from that part of the circle $|s|=M^2-\mu^2$ for which $|\text{arg}s|>66°$, and from the cut $-\infty\leqslant s\leqslant 0$. The two $\pi-\pi$ terms come from the arc $|\text{arg}s|\leqslant 66°$ of the circle. These five terms can be regarded as the contributions to the scattering amplitudes from the various interactions which give rise to low energy $\pi-N$ scattering. Those with small (large) values of $|F|$ correspond to interactions with short (long) ranges. The rescattering term is the contribution to Re$p_{2T,2J}$ from the physical cut $(M+\mu)^2\leqslant s\leqslant\infty$. It is very small except in the case of p_{33} where it is large and varies rapidly.

Several interesting deductions can be made as to the causes of p-wave $\pi-N$ scattering.

(a) For p_{33} at low energies[84] (lab energy $\lesssim$250 MeV) the crossed integral and the $T=1$ $\pi-\pi$ interaction[85] are unimportant. The Born term gives a strong long-range attraction, and the core gives a modest short-range attraction. The $T=0$ $\pi-\pi$ interaction gives an attraction which is more than twice as large as the core term at threshold and even at 250 MeV is bigger than the core term. Therefore any theory which attempts to obtain the position of the $(\frac{3}{2},\frac{3}{2})$ resonance from first principles, must allow for the strong $T=0$ $\pi-\pi$ attraction as well as the short-range (core) attraction.

(b) At threshold the dominant term for p_{11} is the strong long-range Born repulsion. The crossed integral, the core, and the two $\pi-\pi$ interactions all give moderate size attractive terms. The fact that the magnitude of the Born term falls off more rapidly with increasing energy than these other terms explains why the large scattering length $a_{11}=-0.104$ is consistent with the much smaller value Re$p_{11}=-0.024$ found at 98 MeV. Similarly it is easy to understand why α_{11} changes sign and becomes positive before 200 MeV is reached.

(c) The two amplitudes p_{31} and p_{13} have long been known to be very similar in behavior at low energies.[86] From Table III we see that their long-range Born terms, $T=0$ $\pi-\pi$ terms, crossed integrals, and core terms are almost identical at low energies. The only appreciable difference is that the $T=1$ $\pi-\pi$ term (which is repulsive for p_{31} and p_{13}) is three times as large in the case of p_{31} as it is for p_{13}. This causes the scattering length a_{31} to be slightly more negative than a_{13} [$a_{31}=-0.040$, $a_{13}=-0.030$, by Eq. (16)]. The fact that about half of the long-range Born repulsion is cancelled by the $T=0$ $\pi-\pi$ attraction is the main reason for the smallness of the phase shifts α_{31} and α_{13} in the low-energy region.

(iv) Charge Independence

Charge independence appears to be well satisfied (experimentally) for $\pi-N$ scattering, at least up to 400 MeV,[9] but charge independence has not been proved for processes like $\pi+\pi\to N+\bar{N}$ or $\pi+\pi\to\pi+\pi$. We shall examine to what extent our analysis depends on assuming charge independence for the latter processes.

The $\pi-N$ scattering amplitude is, in the notation of I,

$$T=-A+i\gamma\cdot QB, \tag{86}$$

where A, B are the invariant amplitudes. We used throughout the $(\pm)$ charge combinations. These are given by

$$T^{(\pm)}=\tfrac{1}{2}(T_-\pm T_+), \tag{87}$$

where $T_\pm$ are the scattering amplitudes for $\pi^\pm+p\to\pi^\pm+p$ (upper sign to go with upper sign, etc.). Low's relation[87] which enables us to cross from the physical cut $(M+\mu)^2\leqslant s\leqslant\infty$ to the cut $0\leqslant s\leqslant(M-\mu)^2$ can easily be expressed in terms of T_+ and T_- (without any use of charge independence notation). On crossing this gives $T^{(+)}\to T^{(+)}$ and $T^{(-)}\to -T^{(-)}$, and using (86) this gives $A^{(\pm)}\to\pm A^{(\pm)}$, $B^{(\pm)}\to\mp B^{(\pm)}$. These are just the relations which were used in our calculation of the crossed integral terms, and they do not depend on assuming charge independence.

On going over to the third channel ($\pi+\pi\to N+\bar{N}$) we note that by the usual substitution law of relativistic quantum field theory $\pi^\pm+p\to\pi^\pm+p$ are both related to $\pi^++\pi^-\to p+\bar{p}$. It is easy to see that $T^{(+)}$ and $T^{(-)}$ are related to $\pi^+\pi^-$ states having charge conjugation quantum number $C=+1$ and -1, respectively. So $T^{(+)}$ $(T,^{(-)})$ are related to states $\pi^++\pi^-\to p+\bar{p}$ having even (odd) angular momentum J.

If we do not assume charge independence, then G invariance may not be true, and this may affect the unitarity assumptions made in solving equations like (17) for the helicity amplitudes for $\pi+\pi\to N+\bar{N}$. For the $T^{(+)}$ case we saw that the $J=0$ state in this channel was dominant [Sec. 3(iv)], so our pair $\pi^+\pi^-$ is in a 0^+ state. Since there is no 0^+ state with three pions, the unitarity relation between $\langle\pi\pi|N\bar{N}\rangle$ and $\langle\pi\pi|\pi\pi\rangle$ still holds over the range $4\mu^2\leqslant t\leqslant 16\mu^2$. For the $T^{(-)}$ case our $\pi^+\pi^-$ pair is in a 1^- state, and there is a $1^-\pi^+\pi^0\pi^-$ state. Here the unitarity relation need only be valid for $4\mu^2\leqslant t\leqslant 9\mu^2$.

Thus if we do not assume charge independence for the $\pi+\pi\to N+\bar{N}$ channel (or for high-energy processes

[83] In the case of Rep_{33} the crossed integral at $s=(M+\mu)^2$ is made up of 0.002 due to α_{33}, and -0.001 due to α_{11}, α_{31}, α_1, and α_3.

[84] In this section "energy" means lab pion energy. "Low energy" is used to mean lab energy $\leqslant$250 MeV.

[85] S. C. Frautschi and J. D. Walecka, Phys. Rev. **120**, 1486 (1960) have pointed out that the $T=1$ $\pi-\pi$ interaction is small in the p_{33} case.

[86] See for example, F. H. Harlow and B. A. Jacobsohn, Phys. Rev. **93**, 333 (1954).

[87] See, for example, J. Hamilton, *Theory of Elementary Particles* (Oxford University Press, New York, 1959), p. 328.

in the other channels), our deductions from $\pi-N$ scattering about the $T=0$, $J=0$ $\pi-\pi$ phase shift δ_0^0 remain valid, but our conclusions about $T=1$, $J=1$ $\pi-\pi$ scattering may be modified.

(v) Validity of the Mandelstam Representation

The observed s- and p-wave $\pi-N$ data give the six discrepancies $\Delta^{(+)}(s)$ and $\Delta^{(-)}(s)$ on the physical cut $s\geqslant(M+\mu)^2$ and the crossed cut $s\leqslant(M-\mu)^2$. In Secs. 2, 3, and 4 we showed in a variety of ways that the behavior of these discrepancies was of the same general form as we would expect from $\pi-\pi$ interactions contributing via the front part of the circle $|s|=(M^2-\mu^2)$ (Fig. 1). If the Mandelstam representation for $\pi+N\rightarrow\pi+N$ were not valid, there could be other poles and cuts in the s-plane besides those shown in Fig. 1. If such singularities had a strong effect anywhere near the points $s=(M\pm\mu)^2$ we would not expect our analysis to show the self-consistency just mentioned.

Further, the s-wave and both p-wave discrepancies are (reasonably well) fitted by the same $T=0$, $J=0$ and $T=1$, $J=1$ $\pi-\pi$ interactions, and these interactions are in fairly good agreement with other (experimental) information about the $\pi-\pi$ interactions. This provides some proof of the validity of the substitution law which is used to go over to the channel $\pi+\pi\rightarrow N+\bar{N}$, and the validity of the unitary relation between $\langle\pi\pi|N\bar{N}\rangle$ and $\langle\pi\pi|\pi\pi\rangle$ (this is particularly so in the $T=0$ case).

ACKNOWLEDGMENTS

We are indebted to Dr. W. S. Woolcock for information on $\pi-N$ phase shifts and for permission to reproduce Figs. 4, 5, and 7. We are grateful to D. Atkinson, Dr. C. Lovelace, and Dr. T. D. Spearman for comments and discussion.

The following authors wish to express their gratitude for scholarships and maintenance grants: P.M. to the U. S. Air Force, European Office, for a maintenance grant; G.C.O. to the University of London Scholarships Committee for a Studentship; L.L.J.V. to D.S.I.R. for a Research Studentship.

APPENDIX I. PROPERTIES OF THE DENOMINATOR FUNCTIONS $D(\nu)$

Integration of Eq. (41) in Sec. 3(vii) gives

$$\mathrm{Re}D(\nu)=1+\frac{\Gamma}{\pi}\left[\frac{F(\nu)-F(\nu_1)}{\nu-\nu_1}-F'(\nu_1)\right],$$

where

$$F(\nu)=x\ln\left|\frac{1+x}{1-x}\right| \quad \text{for} \quad \nu>0 \quad \text{and} \quad \nu<-1$$

$$=(2/y)\arctan y \quad \text{for} \quad -1<\nu<0.$$

Here

$$x=[\nu/(\nu+1)]^{1/2};\quad y=[(\nu+1)/(-\nu)]^{1/2}.$$

By simple algebra it can be seen that

$$F(\nu)\rightarrow\ln(-4\nu) \quad \text{as} \quad \nu\rightarrow-\infty,$$
$$F(0)=0,$$
$$F(\nu)\rightarrow\ln(4\nu) \quad \text{as} \quad \nu\rightarrow+\infty.$$

Also

$$F'(\nu)\rightarrow 0 \quad \text{as} \quad \nu\rightarrow-\infty,$$
$$F'(\nu)\rightarrow-\infty \quad \text{as} \quad \nu\rightarrow-0,$$
$$F'(\nu)\rightarrow 2 \quad \text{as} \quad \nu\rightarrow+0,$$
$$F'(\nu)\rightarrow 0 \quad \text{as} \quad \nu\rightarrow+\infty.$$

Further, $F'(\nu)<0$ and $F''(\nu)<0$ on $-\infty<\nu<0$ and $F'(\nu)>0$ on $0<\nu<\infty$. These relations are sufficient to establish the properties of $D(\nu)$ which were used in Sec. 3(vii). The function $D(\nu)$ used in Sec. 3(x), Eq. (61) for the case $N(\nu)=\alpha_0$ is readily seen to be given by

$$\mathrm{Re}D(\nu)=1+(\alpha_0/\pi)F(\nu).$$

The properties of $D(\nu)$ used in Sec. 3(x) follow directly.